AD_____

Award Number: DAMD17-98-1-8307

TITLE: Targeting Breast Cancer With Anti HER2/neu Diabodies

PRINCIPAL INVESTIGATOR: Louis M. Weiner, M.D.

CONTRACTING ORGANIZATION: Fox Chase Cancer Center
Philadelphia, Pennsylvania 19111

REPORT DATE: July 2001

TYPE OF REPORT: Annual

PREPARED FOR: U.S. Army Medical Research and Materiel Command
Fort Detrick, Maryland 21702-5012

REPORT DOCUMENTATION PAGE

Form Approved
OMB No. 074-0188

1. AGENCY USE ONLY (Leave blank)	2. REPORT DATE	3. REPORT TYPE AND DATES COVERED
	July 2001	Annual (22 Jun 00 - 21 Jun 01)

4. TITLE AND SUBTITLE
Targeting Breast Cancer With Anti HER2/neu Diabodies

5. FUNDING NUMBERS
DAMD17-98-1-8307

6. AUTHOR(S)
Louis M. Weiner, M.D.

7. PERFORMING ORGANIZATION NAME(S) AND ADDRESS(ES)
Fox Chase Cancer Center
Philadelphia, Pennsylvania 19111

E-Mail: LM_Weiner@fccc.edu

8. PERFORMING ORGANIZATION REPORT NUMBER

9. SPONSORING / MONITORING AGENCY NAME(S) AND ADDRESS(ES)
U.S. Army Medical Research and Materiel Command
Fort Detrick, Maryland 21702-5012

10. SPONSORING / MONITORING AGENCY REPORT NUMBER

11. SUPPLEMENTARY NOTES

12a. DISTRIBUTION / AVAILABILITY STATEMENT
Approved for Public Release; Distribution Unlimited

12b. DISTRIBUTION CODE

13. Abstract ***(Maximum 200 Words)*** *(abstract should contain no proprietary or confidential information)*

The objective of this proposal is to develop new therapeutic reagents for breast cancer. It is our hypothesis that improved diabody-based molecules with affinity for HER2/*neu* can be engineered and will prove to be effective vehicles for the radioimmunotherapy (RAIT) of breast cancer. The first Technical Objective (T.O.) focuses on the optimization of the production of the selected diabody and the identification of the optimal radionuclide and labeling strategy for diabody-based RAIT. This T.O. also involves an investigation into the impact on diabody targeting and RAIT of a variety of factors likely to be encountered in a clinical setting. These include the degree of antigen density, the route (i.v. bolus or continuous infusion) and frequency of administration, the presence of disseminated disease, and the effect of antigen expression on normal tissues. Completion of these experiments will set the stage for proceeding to the clinical evaluation of diabody-based targeting of breast cancer in our second Technical Objective. The clinical component of this proposal (to be initiated in year 3) will entail a Phase I radioimmunoimaging and radioimmunoguided surgery trial designed to elicit information on the dosimetry, specificity and tumor penetration properties of radiolabeled C6.5 diabody, and will assess the RAIT potential of this molecule.

14. Subject Terms (keywords previously assigned to proposal abstract or terms which apply to this award)
Antibodies, diabodies, single-chain Fv fragments, radioimmunotherapy, radioimmunoimaging, yttrium-90, iodine-131, astatine-211, preclinical therapy studies.

15. NUMBER OF PAGES
25

16. PRICE CODE

17. SECURITY CLASSIFICATION OF REPORT	18. SECURITY CLASSIFICATION OF THIS PAGE	19. SECURITY CLASSIFICATION OF ABSTRACT	20. LIMITATION OF ABSTRACT
Unclassified	Unclassified	Unclassified	Unlimited

Table of Contents

INTRODUCTION:

The objective of this proposal is to develop new therapeutic reagents for breast cancer. It is our hypothesis that improved diabody-based molecules with affinity for HER2/*neu* can be engineered and will prove to be effective vehicles for the radioimmunotherapy (RAIT) of breast cancer. The first Technical Objective (T.O.) focuses on the optimization of the production of the selected diabody and the identification of the optimal radionuclide and labeling strategy for diabody-based RAIT. This T.O. also involves an investigation into the impact on diabody targeting and RAIT of a variety of factors likely to be encountered in a clinical setting. These include the degree of antigen density, the route (i.v. bolus or continuous infusion) and frequency of administration, the presence of disseminated disease, and the effect of antigen expression on normal tissues. Completion of these experiments will set the stage for proceeding to the clinical evaluation of diabody-based targeting of breast cancer in our second Technical Objective. The clinical component of this proposal (to be initiated in year 3) will entail a Phase I radioimmunoimaging and radioimmunoguided surgery trial designed to elicit information on the dosimetry, specificity and tumor penetration properties of radiolabeled C6.5 diabody, and will assess the RAIT potential of this molecule.

BODY

Key Research Accomplishments (Year 3):

During the third year of this award we have continued to optimize diabody-based RAIT, with particular emphasis placed on understanding the properties of the diabody and identifying the optimal therapeutic radioisotope partner. The accomplishment in this area was the performance of the first preclinical therapy study employing the short-lived radioisotope astatine-211 (^{211}At) conjugated to an engineered antibody-based molecule. This study (described in detail below) demonstrated the efficacy of treating solid tumors with ^{211}At-conjugated diabody molecules.

Project Milestones (Year 3):

- *Determined that repetitive administrations of unconjugated C6.5 diabody do not impact the growth of established tumors.* Many antibodies employed in tumor therapy exhibit an anti-tumor effect independent of any effector molecules or isotopes that are conjugated to them. Examples include Herceptin (anti-HER2/neu), Rituxin (anti-CD-20) and ABX-EGF (anti-EGFR). In order to prepare for clinical trials it is critical that we evaluate the impact of the C6.5 diabody on tumors overexpressing the HER2/neu target. This is particularly important as therapeutic efficacy of the unconjugated diabody could indicate the potential for a targeted effect on normal tissues that express the HER2/neu antigen. This study employed immunodeficient mice bearing established MDA-MB-361 DYT2 tumors (mean volumes = 557 mm^3 and 684 mm^3 for the treatment and control groups, respectively at the time of first treatment). The 10 mice in the treatment group received 200 μg of unlabeled C6.5 diabody every three days for a total of 21 days while the 10 mice in the control group

were left untreated. Tumor measurements were taken every three days and the mice were examined for signs of toxicity (e.g., weight loss). In this study we found that repetitive high dose C6.5 diabody treatment was not associated with any signs of efficacy or toxicity (figure 1). Accordingly, it is our belief that all therapeutic results we observe in the radioimmunotherapy studies are due to the targeted delivery of radioactive particles by the diabody.

Figure 1,

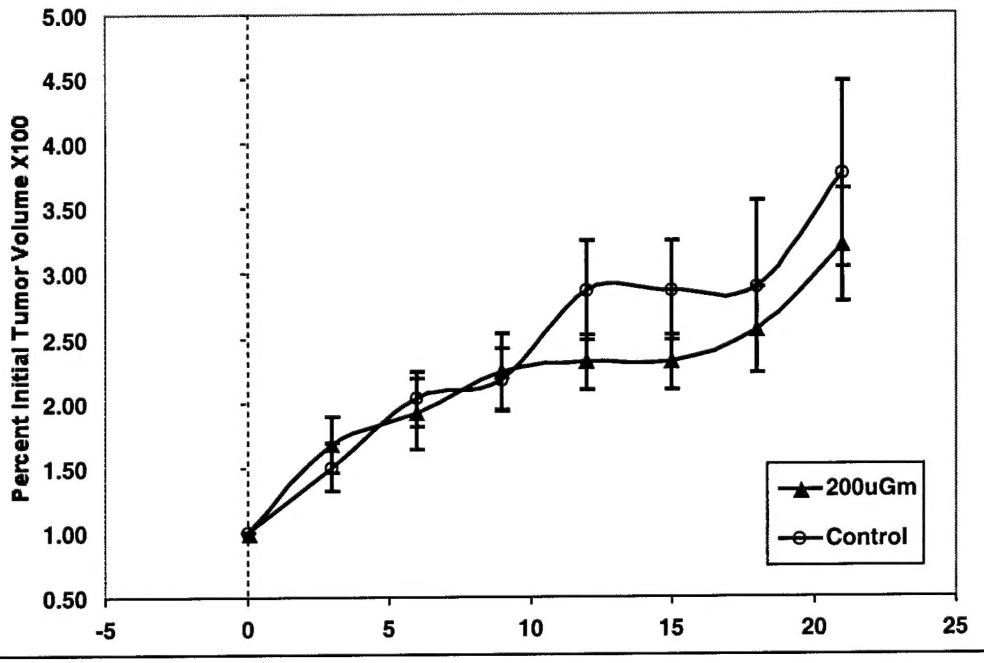

• *Completed the preclinical therapy studies determining the MTD of ^{90}Y-CHX-A"-C6.5 diabody.* In Year Two we identified a new preclinical model for the RAIT studies. This model employs the MDA-MB-361 DYT2 human breast carcinoma cell line which exhibits a rapid rate of growth and internalizes HER2/neu in response to the binding by the C6.5 diabody. We have now performed a number of therapy studies in this model, treating multiple groups of mice with doses of ^{90}Y-CHX-A"-C6.5 diabody ranging from 50 μCi to 500 μCi. Using the method of DeNardo et. al. (Cancer 73; 1994, 1012-1022), we have analyzed these results to determine the LD_{10} and LD_{50} values for ^{90}Y-CHX-A"-C6.5 diabody. The LD_{10} was determined to be 270 μCi and the LD_{50} was found to be 425 μCi.

• *Evaluated the efficacy of treating nude mice bearing established (solid) MDA-MB-361 DYT2 tumors with ^{90}Y-CHX-A"-C6.5 diabody at the MTD.* Preclinical RAIT studies were performed in nude mice bearing established s.c. MDA-MB-361 DYT2 tumors on their abdomen. Cohorts of 10 mice were treated 90 μCi, 150 μCi or 200 μCi (approximately the MTD) of ^{90}Y-CHX-A"-C6.5 diabody or unlabeled C6.5 diabody. The

mice were then observed (tumor volumes measured and weights taken) every three days until the tumors exceeded 10% of their body weight. In this study, efficacy increased with raising dose, with the greatest therapeutic effect observed in the 200 μCi dose group (Figure 2 displays a comparison of the 200 μCi and control groups). This study indicated that significant therapeutic effects can be achieved with ^{90}Y-CHX-A" C6.5 diabody. These results are currently being used as the basis for discussions on initiating a clinical trial with ^{90}Y-CHX-A" C6.5 diabody.

Figure 2. ^{90}Y-CHX-A" C6.5 diabody RAIT of immunodeficient mice bearing established MDA-MB-361 DYT2 breast carcinoma tumors. A single i.v. dose containing 200 μCi of yttrium-90 displayed significant reduction in the rate of tumor growth as compared to mice treated with unlabeled C6.5 diabody. N=10 mice per group, standard deviation of the means are indicated.

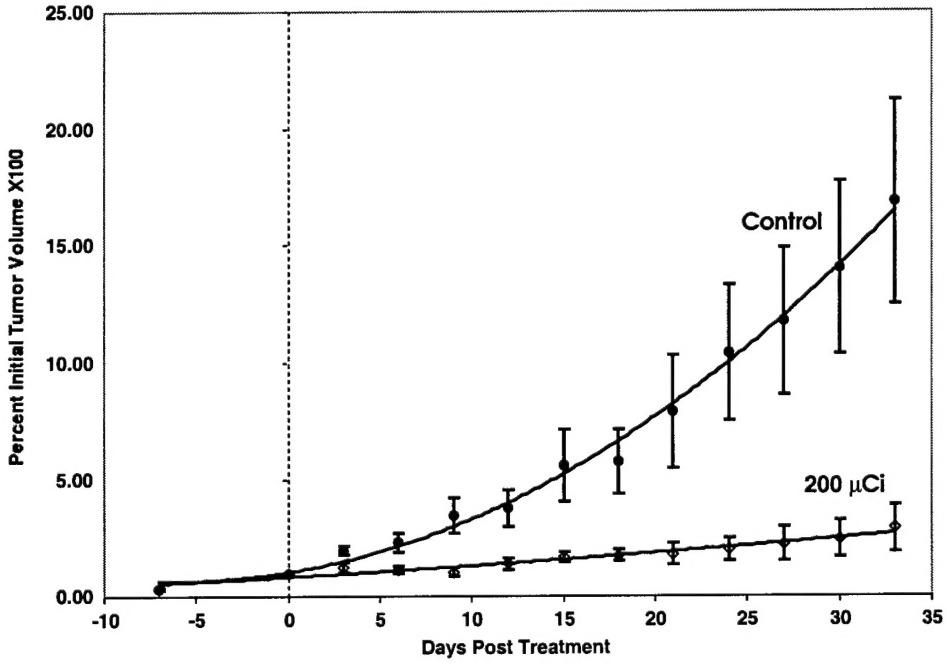

- *Initiated preclinical therapy studies evaluating the efficacy of ^{211}At-C6.5 diabody therapy of established tumors in nude mice.* Alpha particles have a short track length (approx. one cell in diameter). However over the course of this track length they deliver exponentially greater energy than that delivered by a beta particle. In the nucleus this high energy leads to unrepairable double stranded breaks in DNA (beta particles cause repairable single strand breaks). As such, a single alpha particle can lead to the death of a tumor cell. In general, alpha particles are emitted from radioisotopes that are too short-lived for pairing with intact antibodies. However, the 7 hour half-life of one particular alpha particle-emitting radioisotope, ^{211}At, is ideally suited for the pharmacokonetics of the C6.5 diabody. *N*-succinimidyl *N*-(4-[^{211}At]astatophenethyl) succinimate (^{211}At-SAPS) was produced by our collaborators, Drs. Brechbiel and Waldmann of the National Cancer Institute. The compound was

shipped to our lab where it was conjugated to the C6.5 diabody. In this initial study, cohorts of 8 mice were treated with 10 or 25 μCi of ^{211}At-SAPS-C6.5 diabody, or unlabeled C6.5 diabody. These doses were selected as studies performed by our collaborators with intact antibody-conjugates determined that 10 μCi was the MTD and 25 μCi was found to lead to significant toxicity in mice. After treatment, our mhe mice were observed for toxicity and therapeutic efficacy as described above. Both treatment groups showed no signs of significant toxicity and both were associated with dramatic therapeutic effects (Figure 3). Future studies will focus on determining the MTD of ^{211}At-SAPS-C6.5 diabody and will evaluate the importance of internalization on therapeutic efficacy.

Figure 3. ^{211}At-conjugated C6.5 diabody therapy of mice bearing established MDA-MB-361 DYT2 tumors. Cohorts of 8 mice were treated with a single dose of 10 or 25 μCi of ^{211}At-SAPS-conjugated C6.5 diabody, or unlabeled C6.5 diabody. Tumor volumes are plotted as a percent of the initial volume of each tumor at time of treatment. Standard errors of the mean are indicated.

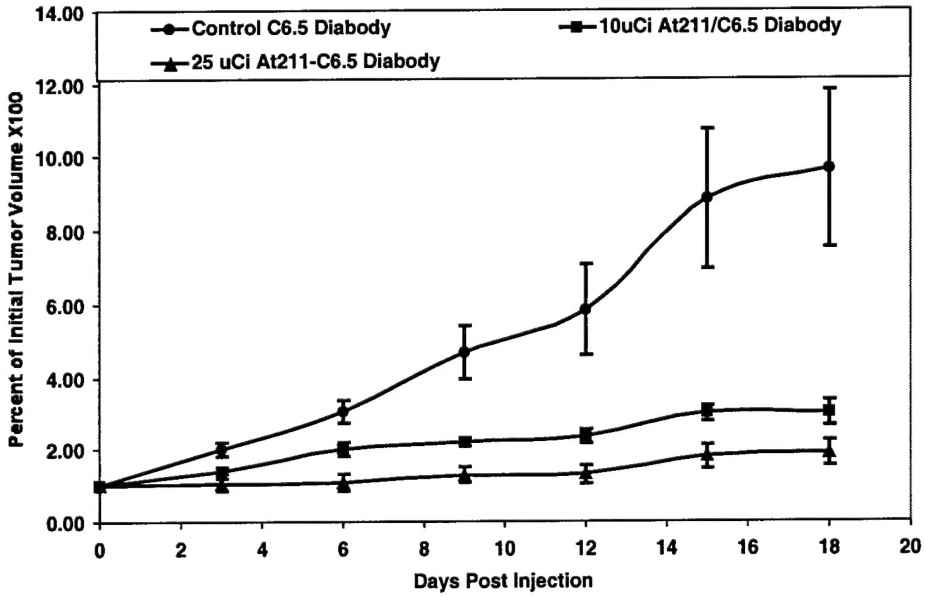

- A critical focus of grant is to evaluate the C6.5 diabody in a phase I clinical trial. We have spent significant efforts over the course of this award attempting to identify a source for GMP diabody for the clinical trial. Initial discussions were carried out with Neoprobe Inc., a company focused on hand-held gamma probes for radioguided surgery. However, the company underwent a difficult financial period and was unable to provide support for this work. We have also approached a number of other companies involved in antibody-based therapeutics, including NeoRx, Amgen, Nordion, etc. As a result of these discussions, it has become very apparent to us that we will need to develop the diabody ourselves. Accordingly, we have acquired estimates for GMP production and sterile fill from a GMP production facility at the University of Iowa. Based upon these estimates we have prepared and submitted an application for a DOD Clinical Bridge Award to support the production of GMP

grade C6.5 diabody for the above phase I clinical trial. A clinical trial protocol has also been prepared and work will begin on the preparation of an IND application this summer.

REPORTABLE OUTCOMES:

Publications That Emanated From This Grant:

- Manuscripts:

Adams, G.P., Shaller, C.C., Chappel, L. Wu, C., Horak, E.M., Simmons, H.H., Litwin, S., Marks, JD., Weiner, L.M. and Brechbiel, M.W. Delivery of the alpha-emitting radioisotope Bi-213 to tumors via single-chain and diabody molecules. Nucl. Med. Biol., 27:339-346, 2000.

Nielsen, U.B., Adams, G.P., Weiner, L.M. and Marks, J.D.. Targeting of bivalent anti-HER2/*neu* diabody antibody fragments to tumor cells is independent of the intrinsic antibody affinity. Cancer Research, 60:6434-6440, 2000.

Adams, G.P., Shaller, C.C., Dadachova, K., Simmons, H.H., Horak, E.M., Marks, J., Brechbiel, M.W., and Weiner, L.M. Treatment of Established Human Tumor Xenografts in Mice with ^{90}Y-CHX-A" C6.5 Diabody (In preparation).

- Abstracts/Presentations:

Adams, G.P. Tumor targeting and Radioimmunotherapy with single-chain Fv and diabody molecules. Oral presentation at the 17th International Conference on Advances in the Application of Monoclonal Antibodies in Clinical Oncology., June 2000, Samos, Greece.

Adams, G.P., Shaller, C.S., Horak, E.M., Simmons, H.H., Dadachova, K., Chappell, L.L., Wu, C., Marks, J.D., Brechbiel, M.W. and Weiner, L.M. Radioimmunotherapy of established solid tumor xenografts with alpha and beta emitter-conjugated antiHER2/neu single-chain Fv and diabody molecules. Oral presentation at the Eighth Conference on Radioimmunodetection and Radioimmunotherapy of Cancer (Princeton, N.J.) Cancer Biotherapy & Radiopharmaceuticals, 15:402, 2000.

Adams, G.P. Single-chain Fv and Diabody Molecules: Tumor Targeting Properties and Radioimmunotherapy Studies. Presented at the First China International Symposium on Antibody Engineering: Technology and Applications (Tianjin, China) September 2000.

Adams, G.P. Effects of Antibody Structure and Affinity on Tumor Targeting and Penetration. Presented at IBC's 11th Annual International Conference on Antibody Engineering (La Jolla, CA), December 2000.

Adams, G.P. Tumor targeting and Radioimmunotherapy with single-chain Fv and diabody molecules. 18th International Conference on Advances in the Application of Monoclonal Antibodies in Clinical Oncology. June 2001, Vouliagmeni, Greece.

CONCLUSIONS:

Over the past year we have continued our efforts to optimize C6.5 diabody-based RAIT. We have determined that yttrium-90 is an excellent partner and have preliminary information that astatine-211 may be even better. While we will continue our work to evaluate astatine-211, we feel that yttrium-90 based therapy has demonstrated sufficient efficacy to justify the initiation of a phase I clinical trial. Accordingly we are attempting to secure funding for the production of GMP diabody.

ACRONYMS AND ABREVIATIONS

CD-20	A cell surface protein present on B-cells and B-cell lymphomas.
CHX-A"	A chelating agent capable of binding radiometals to a protein
EGFR	Epidermal Growth Factor receptor
HER2/neu	A protein of the Epidermal Growth Factor receptor family
MTD	Maximum tolerated dose
%ID/g	Percentage of the injected dose localized per gram of tissue
RAID	Radioimmunodetection
RAIT	Radioimmunotherapy
RIGS	Radioimmunoguided surgery
ScFv	Single-chain Fv molecule
SEM	Standard error of the mean

Appendix

1. Nielsen UB, Adams GP, Weiner LM, Marks JD: Targeting of Bivalent Anti-ErbB2 Diabody Antibody Fragments to Tumor Cells Is Independent of the Intrinsic Antibody Affinity. Cancer Research 60,6434-6440, November 15, 2000.
2. Adams GP, Shaller CC, Chappell LL, Wu C, Horak EM, Simmons HH, Litwin S, Marks JD, Weiner LM, Brechbiel MW: Delivery of the α-Emitting Radioisotope Bismuth-213 to Solid Tumors via Single-Chain Fv and Diabody Molecules. Nuclear Medicine & Biology, Vol. 27, pp. 339-346, 2000.

[CANCER RESEARCH 60, 6434–6440, November 15, 2000]

Targeting of Bivalent Anti-ErbB2 Diabody Antibody Fragments to Tumor Cells Is Independent of the Intrinsic Antibody Affinity[1]

Ulrik B. Nielsen, Gregory P. Adams, Louis M. Weiner, and James D. Marks[2]

Department of Anesthesiology and Pharmaceutical Chemistry, University of California, San Francisco, California 94110 [U. B. N., J. D. M.], and Department of Medical Oncology, Fox Chase Cancer Center, Philadelphia, Pennsylvania 19111 [G. P. A., L. M. W.]

ABSTRACT

In immunodeficient mice antitumor single-chain Fv (scFv) molecules penetrate tumors rapidly and have rapid serum clearance, leading to excellent tumor:normal organ ratios. However, the absolute quantity of scFv retained in the tumor is low due to rapid serum clearance and monovalent scFv binding. We previously demonstrated that the presence of an additional binding site prolongs *in vitro* and *in vivo* association of scFv-based molecules with tumor cells expressing relevant antigen. The contribution of the intrinsic affinity of each component scFv to the association between a dimeric scFv and its target antigen is largely unknown. Here, we have constructed bivalent diabody molecules from three affinity mutants of the human anti-ErbB2 (HER2/*neu*) scFv molecule C6.5 by shortening the peptide linker between the heavy (V_H) and light (V_L) chains variable domains from 15 to 5 amino acids. The shorter linker prevents intramolecular pairing of V_H and V_L, resulting in intermolecular pairing and creation of a dimeric M_r 50,000 molecule with two antigen-binding sites. The scFv used to create the diabodies span a 133-fold range of affinity for the same epitope of ErbB2 [133 nM (C6G98A), 25 nM (C6.5), and 1 nM (C6ML3–9)] and differ by only one to three amino acids. Diabody binding kinetics were determined by surface plasmon resonance on the immobilized ErbB2 extracellular domain. The association rate constants obtained for each diabody molecule were similar to that of the parental (component) scFv. However, the dissociation rate constants obtained for the bivalent diabodies were up to 15-fold slower. The magnitude of the decrease in the bivalent dissociation rate constant was inversely proportional to the monovalent interaction, ranging from only 3-fold for that of the C6ML3–9 diabody to 15-fold for the C6G98A diabody. This resulted in only a 22-fold difference in bivalent affinity, compared with a 133-fold difference in affinity for the respective scFv. Equilibrium-binding constants obtained by surface plasmon resonance correlated well with the equilibrium-binding constants determined *in vitro* on ErbB2 overexpressing cells. Biodistribution studies were performed in *scid* mice bearing established SKOV3 tumors. At 24 h, 3–37-fold more diabody was retained in tumor compared with the parental scFv monomers. This likely results from a higher apparent affinity, because of bivalent binding, and a slower serum clearance. Surprisingly, the differences in affinity between diabodies did not result in differences in quantitative tumor retention or tumor to blood ratios. In fact, the diabody constructed from the lowest affinity scFv exhibited the best tumor-targeting properties. We conclude that, above a threshold affinity, other factors regulate quantitative tumor retention. In addition, straightforward dimerization of a low-affinity scFv leads to significantly greater tumor localization than does exhaustive scFv affinity maturation.

INTRODUCTION

Mab[3]-based radioimmunotherapy of solid tumors has been hindered by the physical characteristics of IgG molecules. With a molecular weight of ~M_r 155,000, these molecules exhibit both a slow diffusion into tumors and a slow elimination from circulation. The former property leads to heterogeneous delivery into tumors, whereas the latter property results in dose-limiting myelotoxicity. Recent advances in antibody-engineering technology has led to the development of scFv molecules, composed of the variable light (V_L) and heavy (V_H) domains of an immunoglobulin molecule (1, 2). These small scFv molecules currently represent the minimal antibody-based construct capable of specifically interacting with antigen without excessive cross-reactivity. In both mice and patients their size leads to a rapid renal elimination, yielding excellent tumor:normal organ ratios and lower nonspecific background, as compared with intact IgG antibodies (3–5). In addition, the scFv penetrates more deeply into poorly vascularized regions of tumors than do the Fab′, F(ab′)$_2$, and intact IgG (6). However, the monovalent nature and rapid renal clearance of the scFv results in the specific retention of only small quantities in the tumors in immunodeficient mice with rarely >1%ID localized per gram of tumor at 24 h after injection (5–8). We have recently examined the tumor-targeting properties of a series of scFv mutants that vary in affinity for the same epitope of the tumor antigen ErbB2. In this model, the 24-h tumor retention of a scFv with an affinity of 133 nM (C6G98A) was indistinguishable from that achieved with an irrelevant scFv. Increasing the affinity to 25 nM (C6.5) and 1 nM (C6ML3–9) resulted in significantly greater tumor retentions of 0.8%ID/g and 1.4%ID/g, respectively (9).

We, and others, have investigated the use of larger, multivalent, scFv-based constructs to improve the degree and specificity of *in vivo* targeting of solid tumors (5, 10–13). In general, increasing the number of antigen binding sites has led to enhanced tumor retention, as compared with that achieved with monovalent scFv molecules. One of the more promising scFv-based molecules is a noncovalent dimer or diabody (14). Diabodies are constructed by shortening the scFv peptide linker from 15 aa to 5 aa. The shorter linker does not permit pairing of the V_H and V_L domains on the same polypeptide chain, forcing pairing between complementary domains of two different chains. The resulting molecule has two antigen-binding sites at opposite ends of the molecule, separated by ~65 Å (15). We have previously reported on the construction of a diabody from the C6.5 scFv, which specifically recognizes ErbB2. In tumor-bearing mice the C6.5 diabody exhibited a >7-fold increase in tumor retention without the loss of targeting specificity (16). To date, however, the relative impact of increased size, increased valance, and the affinity of the parental scFv molecules on the tumor-targeting properties of scFv dimers has yet to be elucidated.

In this study, we analyze the importance of intrinsic antibody affinity on the *in vitro* and *in vivo* targeting of ErbB2 overexpressing tumor cells using a series of diabodies constructed from the three

Received 3/27/00; accepted 9/13/00.

The costs of publication of this article were defrayed in part by the payment of page charges. This article must therefore be hereby marked *advertisement* in accordance with 18 U.S.C. Section 1734 solely to indicate this fact.

[1] Supported by National Cancer Institute Grants CA65559 and CA06927; Department of Defense Grants DAMD17-98-1-8189, DAMD17-98-1-8307, and DAMD17-94-J-4433; an appropriation from the Commonwealth of Pennsylvania, the Bernard A. and Rebecca S. Bernard Foundation, the Frank Strick Foundation, and the CaPCURE Foundation.

[2] To whom requests for reprints should be addressed, at Department of Anesthesiology and Pharmaceutical Chemistry, San Francisco General Hospital, University of California–San Francisco, Room 3C-38, 1001 Potrero Avenue, San Francisco, CA 94110. E-mail: Marksj@anesthesia.ucsf.edu.

[3] The abbreviations used are: Mab, monoclonal antibody; scFv, single-chain Fv; %ID, percentage of the injected dose; SPR, surface plasmon resonance; RU, resonance unit; ECD, extracellular domain; AUC, area under the curve; aa, amino acid.

affinity variants of the C6.5 anti-ErbB2 scFv (spanning a 133-fold range of affinity) described above. By applying SPR technology to the analysis of antigen binding, the intrinsic as well as apparent bivalent binding kinetics of the three diabodies were determined. Diabody binding to tumor cells was investigated by fluorescence cytometry using the ErbB2-positive breast cancer cell line SKOV3 to estimate equilibrium constants. Finally, biodistribution studies were performed in *scid* mice bearing established SKOV3 tumors.

MATERIALS AND METHODS

ScFv and Diabody Production. The scFv genes used for construction of diabodies were derived from the human scFv C6.5 (17, 18). Diabodies were constructed, as described previously, using a 5-aa linker between the V_H and V_L domains (16) and cloned into pUC119mycHis (17) for expression with COOH-terminal *myc* and hexahistidine epitope tags. For measurement of antibody fragment affinity on cells, the scFv and diabody genes in pUC119mycHis were amplified by PCR using the primer 5′-GCCATGGC-CGACTACAAGGCAAAGCAGGTGCAGCTGGTGCAG-3′, which adds the epitope tag DYKAK (19) recognized by the anti-FLAG M1 antibody (Sigma Chemical Co.) onto the NH_2 terminus of the scFv or diabody. The scFv and diabodies were expressed in *Escherichia coli* strain TG1. Briefly, 0.75 liter of media (2× Tryptone yeast with 100 μg/ml ampicillin and 0.1% glucose) was inoculated with an overnight culture of the appropriate plasmid in TG1, grown to an A_{600} of 0.9 and expression induced by the addition of isopropyl-β-D-thiogalactopyranoside to a final concentration of 0.5 mM. The culture was grown at 30°C for 4 h (for scFv) or overnight (for diabodies).

Cells were harvested by centrifugation (4000 × *g*, 20 min), and the pellets were resuspended on ice for 30 min in periplasmic extraction buffer [30 mM Tris, 2 mM EDTA, and 20% sucrose (pH 8.0)] containing 100 μg/ml DNase. Bacteria were pelleted by centrifugation at 5000 × *g* for 20 min, resuspended in osmotic shock buffer (5 mM $MgSO_4$), and incubated for another 20 min on ice. Bacteria were pelleted (7000 × *g*, 20 min), and supernatants from the periplasmic extraction buffer and $MgSO_4$ fractions combined and cleared by centrifugation at 10,000 *rpm* for 30 min at 4°C. The resulting solution was dialyzed in PBS. All molecules were purified by immobilized metal affinity chromatography (17), followed by size exclusion chromatography on a BioCAD SPRINT fast protein liquid chromatography system (PerSeptive Biosystems) using either a Superdex 75 (for scFv) or a Superdex 200 column (for diabodies). Protein concentrations were determined spectrophotometrically from the absorbance at A_{280} using the extinction coefficient $\epsilon = 1.4$. The C6.5 scFv-Fc fusion protein was expressed from *Pichia pastoris* and purified using protein G affinity chromatography, as described elsewhere (20).

Measurement of Binding by SPR. Association rate constants (k_{on}) were determined using SPR in a BIAcore1000 (BIAcore Inc.). Approximately 500 RU of the ErbB2 ECD were coupled to a CM5 sensor chip as described previously (17), and association rate constants were measured under continuous flow of 15 μl/min using scFv and diabody concentrations ranging from 100-1200 nM. Association rate constants were calculated from a plot of [ln(dR/dt)]/t *versus* concentration of binding sites using the BIAanalysis software (version 2.1). Apparent dissociation rate constants (k_{off}) were determined using the function BIGinjection. Different volumes [600 μl, 330 μl, 100 μl, 50 μl, and 5 μl of diabody or scFv solutions (concentration, 25 μg/ml)] were injected over the CM5 sensor chip (500 RU ECD immobilized) at a flow rate of 5 μl/min. The dissociation rate constants of all molecules were determined at >90% of maximal binding to the chip, with the exception of the C6G98A and C6.5 scFv, which were measured as close to maximal binding as possible (>50%). To determine intrinsic rate constants, diabodies were biotinylated with NHS-LC-biotin (Pierce Chemical Co.) at a biotin:diabody ratio of ~5:1 and as described by the manufacturer. Approximately 5000 RU avidin (Sigma Chemical Co.) was conjugated to a CM5 sensor chip using similar conditions as described for ErbB2 ECD (17). Biotinylated diabody was injected onto the surface to yield ~500 RU diabody bound to the surface. Saturating concentrations of ErbB2 were then injected, and dissociation rate constants were determined immediately following ErbB2 ECD dissociation. To determine their serum stability, diabodies were incubated in 90% human serum at a final concentration of 50 μg/ml for 3 days at 37°C. After diluting 10-fold in running buffer, the binding concentration was determined by SPR using immobilized ErbB2 ECD as described (18) and compared with that of the diabody stock stored at 4°C.

Cell Surface Binding Measurements. Human ovarian carcinoma SKOV3 cells (HTB 77; American Type Culture Collection) that overexpress ErbB2 were grown to 80–90% confluence in RPMI media supplemented with 10% FCS and harvested by trypsinization. Each scFv or diabody was incubated in triplicate with 1×10^5 cells in 96-well plates with V-shaped wells for 2 h at the concentrations indicated. Cell binding was performed at room temperature in PBS containing 2% FCS and 0.1% sodium azide in a total volume of 200 μl. Sodium azide was included in the incubation buffer to minimize receptor internalization. After two washes with 200 μl of PBS, bound scFv or diabody was detected by the addition of 100 μl (10 μg/ml) of FITC-labeled anti-FLAG monoclonal antibody clone M1. After incubating 30 min at room temperature, the cells were washed twice and resuspended in PBS containing 4% paraformaldehyde. Fluorescence was measured by flow cytometry in a FACSort (Becton Dickinson), and median fluorescence (F) was calculated using Cellquest software (Becton Dickinson) and the background fluorescence was subtracted. Equilibrium constants were determined as described (21), except that values were fitted to the equation $1/F = 1/F_{max} + (K_D/F_{max})(1/[scFv])$ using the software program SigmaPlot (SPSS Inc.).

Biodistribution Studies. Diabody and scFv molecules were radiolabeled with ^{125}I using the chloramine T method (^{125}I: protein ratio, 1:10), as described previously (5). The quality and immunoreactivity of the radiopharmaceuticals were evaluated by SDS-PAGE and in a live cell-binding assay as described (5). CB.17 Icr *scid* mice, 6–8 weeks of age, were obtained from the Fox Chase Cancer Center Laboratory Animal Facility. SKOV3 cells (2.5×10^6) were implanted s.c. on the abdomen of each mouse. When the tumors had achieved a size of 50–200 mg (~8 weeks), Lugol's solution was placed in their drinking water to block thyroid accumulation of radioiodine, and biodistribution studies were initiated. Twenty micrograms (100 μl) of radioiodinated diabody or scFv were administered by i.v. tail vein injection to each mouse. Cohorts of five mice that received the ^{125}I-diabodies or scFv were sacrificed at 1, 4, 8 (except C6.5db), 24, 48, and 72 h after injection. The mean and SEM of retention of each radiopharmaceutical in tissue (%ID/g) and blood (%ID/ml) were determined from decay-corrected counts, as described (5). Calculations of the estimated cumulative localization (AUC) of diabody in tumor (% h^{-1} g^{-1}) and blood (% h^{-1} ml^{-1}) were determined using the NCOMP program (22).

RESULTS

Construction, Expression, and Characterization of Recombinant scFv and Diabodies. To determine the impact of intrinsic affinity on the *in vitro* binding and *in vivo* tumor targeting of bivalent diabodies, we constructed diabodies from the scFv C6G98A, C6.5, and C6ML3–9. C6G98A and C6ML3–9 were derived from the C6.5 scFv by site-directed mutagenesis and phage display (18). The three scFv differ from each other by, at most, three amino acids, bind identical epitopes on the ErbB2 ECD and bind with K_D ranging from 1.3×10^{-7} M to 1.0×10^{-9} M (133-fold difference in K_D). Diabodies were constructed by genetically shortening the linker between the scFv from 15 to 5 aa (16). Recombinant diabodies were expressed and purified from the *E. coli* periplasm by immobilized metal affinity chromatography and size exclusion chromatography with yields of 0.5–3 mg/liter of shake flask culture. More than 90% of the purified protein was functional as determined by SPR and size exclusion chromatography in the presence of ErbB2 ECD (results not shown).

***In Vitro* Binding Kinetics of scFv and Diabodies.** The association and dissociation rate constants of the three scFv were remeasured using SPR, and the K_D was calculated as k_{off}/k_{on}. The K_D of the three scFv were comparable with values previously reported and spanned a 133-fold range of affinities (Table 1). Intrinsic diabody association and dissociation rate constants were measured to determine whether construction of diabody molecules affected the antigen binding. The association rate constant was determined by immobilizing the ECD on the sensor chip surface. The intrinsic dissociation rate constants of each diabody were determined by immobilizing biotinylated diabody

Table 1 *Comparison of intrinsic rate and equilibrium constants of scFv and diabodies*

	scFv[a]			Diabody		
Clone	k_{on} [10^5 $s^{-1}M^{-1}$]	k_{off} [10^{-3} s^{-1}]	K_D [10^{-9}M]	k_{on}[b] [10^5 $s^{-1}M^{-1}$]	k_{off}[c] [10^{-3} s^{-1}]	Intrinsic K_D[d] [10^{-9} M]
C6G98A	4.1	55	133	2.3	94	409
C6.5	4.0	10	25	2.6	8.8	34
C6ML3–9	7.6	0.76	1.0	3.9	0.78	2.0

[a] Association and dissociation rate constants for purified scFv were determined by SPR.
[b] Association rate constants (k_{on}) for purified diabodies were determined on immobilized ErbB2 ECD.
[c] Dissociation rate constants (k_{off}) of diabodies were determined by immobilizing diabody and flowing recombinant ErbB2 ECD over the surface (to avoid bivalent binding of diabody affecting the k_{off}).
[d] Equilibrium constants were calculated as $K_D = k_{off}/k_{on}$.

on an avidin-coated sensor chip. Because the recombinant ErbB2 ECD is monomeric in solution (results not shown), by immobilizing the diabody, bivalent binding is not possible and the dissociation rate constant represents that of the monovalent binding. The diabody association rate constant and the intrinsic dissociation rate constant were determined, and the intrinsic equilibrium-binding constants were calculated. These were slightly lower (2–3-fold) than the values measured for the scFv from which they were constructed, mainly as a result of decreased association rate constants (Table 1). Dissociation rate constants were similar to those of the scFv, indicating that the diabody homodimer formation does not significantly alter ligand binding to the individual binding site. The dissociation rate constant for the C6.5 scFv determined by the same approach was similar to what was determined by immobilizing ECD (results not shown).

To evaluate the contribution of the second binding site on the K_D, diabodies were analyzed for binding to immobilized ErbB2 ECD. It was hypothesized that the duration of incubation of diabody with immobilized ErbB2 ECD would affect the dissociation rate because a longer incubation would increase the likelihood of bivalent binding. To determine whether this was true, C6G98A diabody was passed over immobilized ErbB2 ECD for durations of 1–120 min. A flow rate of 5 μl/min was used for these studies because the BIGinject function for the BIAcore1000 instrument is limited by the volume of the injection loop (750 μl) and, thus, does not allow 120-min injections at faster flow rates. Although use of more rapid flow rates (15 μl/min) may minimize rebinding and yield more accurate off rates, the dissociation rate constants obtained for the scFv in this study using the 5-μl/min flow rate are comparable with our previous data using a flow rate of 15 μl/min (Ref. 18; k_{off} of C6G98A scFv = 130×10^{-3} s^{-1} at 15 μl/min *versus* 55×10^{-3} s^{-1} at 5 μl/min; k_{off} for C6.5 = 6.3×10^{-3} s^{-1} at 15 μl/min, *versus* 10×10^{-3} s^{-1} at 5 μl/min; and k_{off} for C6ML3–9 = 0.76×10^{-3} s^{-1} at both flow rates).

As expected, the rate of dissociation decreased with increasing incubation time (Fig. 1*A*). This experiment was repeated for the C6.5 and C6ML3–9 scFv and diabody, and the results were plotted as dissociation rate *versus* incubation time (Fig. 1, *B–D*). In these experiments, the apparent bivalent equilibrium constants of diabodies decreased with increased association time (Fig. 1). For C6ML3–9db, the diabody with the highest intrinsic affinity, the change in dissociation rate was only minimal over the 2-h examination period (Fig. 1*D*). However, for the C6G98Adb, which has the lowest intrinsic affinity, the dissociation rate dropped dramatically during the first 5 min of association and then stabilized (Fig. 1*B*). Similarly, for the C6.5 diabody, the dissociation rate stabilized after about 70 min of association (Fig. 1*C*). These results indicate an inverse relationship between the dissociation rate constant of a bivalent molecule and the time required to achieve bivalent binding.

In these experiments, a diabody concentration of 25 μg/ml was used because this is comparable with the predicted serum concentration in patients following the administration of therapeutic doses of Mab (23) and approximately equal to the calculated diabody dose (20 μg) used in the biodistribution studies described below. Rebinding of the diabody to the antigen matrix on the BIAcore chip will alter the measured dissociation rates. To minimize this effect, diabody dissociation rates were fitted as close to maximum binding as possible. The dissociation rate constants obtained for the C6G98A and C6.5 diabodies after 5 and 70 min of association, respectively, most likely represent the true bivalent equilibrium constants under the conditions studied.

The dissociation rate constants of the diabodies obtained after 2 h of association are reported in Table 2. The diabody apparent equilibrium constants were then calculated as k_{on}/k_{off} (after 2 h of binding; Table 2). Not surprisingly, the apparent affinity was significantly greater than the intrinsic affinity. The magnitude of the increase in affinity, however, was inversely proportional to the intrinsic affinities of the molecules (Tables 1 and 2). For the lowest affinity diabody, C6G98Adb, the increase in affinity mediated by bivalent binding was 51-fold, from 409 nM to 8 nM. Similarly, for the C6.5 diabody the affinity increased 21-fold from 34 nM to 1.6 nM as a result of bivalent binding. For the diabody with the highest affinity, C6ML3–9, the increase in apparent affinity was only 5.6-fold, from 2.0 nM to 0.36 nM. This relationship was also observed when comparing the increase in apparent affinity of the diabody to the affinity of the parental scFv

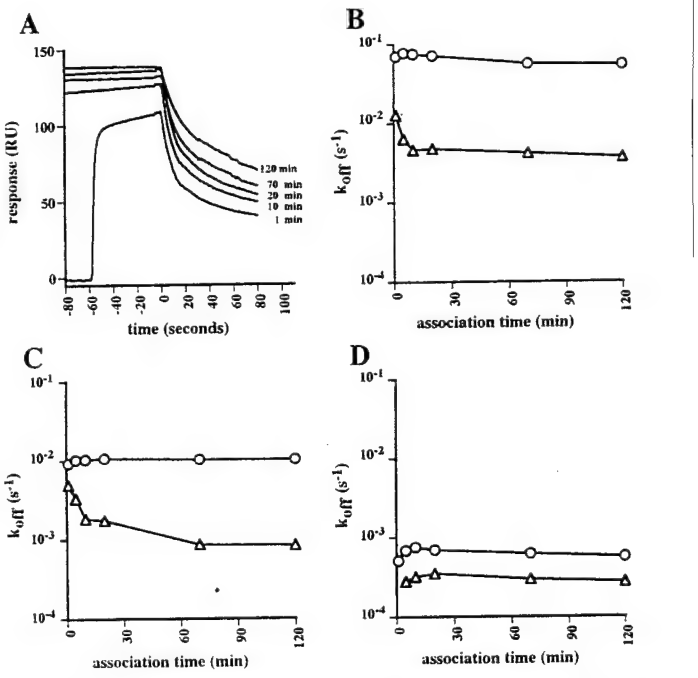

Fig. 1. Effect of association time on the dissociation rate constant (k_{off}) of scFv and diabodies as determined by SPR. *A*, C6G98A diabody (25 μg/ml) was injected at 5 μl/min for the times indicated onto ~1000 RU of ErbB2 ECD immobilized on a BIAcore CM10 chip. *B–D*, dissociation rate constants of diabody (△) or scFv (○) were determined from sensorgrams such as the one in shown in *A* and plotted as a function of time. *B*, C6G98A; *C*, C6.5; *D*, C6ML3–9.

Table 2 *Apparent diabody dissociation rate constants and equilibrium constant*

Diabody dissociation rate constants were measured on immobilized ErbB2 ECD after 2 h of association. Equilibrium constants were calculated as $K_D = k_{off}/k_{on}$.

Diabody	k_{on} $[10^5\ s^{-1}M^{-1}]$	k_{off} (2-h binding) $[10^{-3}\ s^{-1}]$	Apparent K_D $[10^{-9}$ M]	K_D scFv/K_D diabody	Intrinsic K_D diabody/ apparent K_D diabody
C6G98A	4.6	3.7	8.0	17	51
C6.5	5.2	0.84	1.6	16	21
C6ML3–9	7.8	0.28	0.36	2.8	5.6

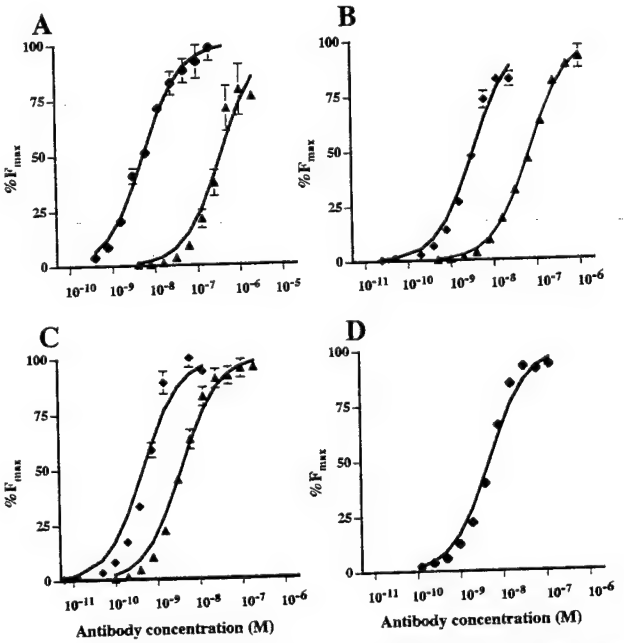

Fig. 2. Equilibrium-binding curves for scFv, diabodies, and C6.5 scFv-Fc fusion protein as determined by flow cytometry. ScFv (▲), diabodies (♦), or C6.5-fusions (◆) were incubated with SK-OV-3 cells at room temperature for 2 h, and binding was detected with anti-FLAG-FITC conjugate: *A*, C6G98A scFv and diabody; *B*, C6.5 scFv and diabody; *C*, C6ML3–9 scFv and diabody; D, bivalent C6.5 scFv-Fc fusion. Experiments were done in triplicate; *bars* represent SDs.

(17-fold, 16-fold, and 2.8-fold for C6G98A, C6.5, and C6ML3–9, respectively; Table 2). Differences between the increment in apparent K_D seen for scFv *versus* diabody are due to minor differences in the intrinsic association and dissociation rate constants that resulted from conversion of the scFv to diabody format (Table 1).

Equilibrium Constants for Binding to ErbB2-overexpressing Cancer Cells. Because the ErbB2 target antigen could be present in many orientations on the BIAcore chip, the K_D determined by SPR may not accurately reflect that measured for cell surface binding to ErbB2. Accordingly, to validate the bivalent apparent equilibrium constants determined by SPR, equilibrium constants were also determined for binding to ErbB2 expressed on the surface of SKOV3 tumor cells using fluorescence cytometry (Fig. 2). Because direct fluorescent labeling of antibody fragments is often associated with decreased affinity, diabodies were genetically tagged with an affinity-matured version of the FLAG tag (DYKAK; Ref. 19) and detected with FITC-labeled anti-FLAG M1. We determined that the affinity of the anti-FLAG antibody for the FLAG peptide tag on the diabody constructs was 2 nM (results not shown) and, thus, was similar to what has previously been published for its interaction with the synthetic peptide (19). This high-affinity interaction ensured that the secondary antibody could be used at saturating concentration. As described by Benedict *et al.* (21), these conditions are required for the measured fluorescence to be directly proportional to the amount of antibody fragment bound.

The results of these studies demonstrated that the scFv and diabody equilibrium constants on cells, as determined by flow cytometry, correlated well with the values determined by SPR (Table 3 and Fig. 2). The correlation indicates that the diabodies, despite their relatively rigid structure (15), are able to bind two ligands on the cell surface simultaneously, as observed in the more artificial SPR analysis. As with the case of equilibrium constants measured by SPR, bivalent diabodies had significantly higher apparent affinities than the parental scFv. Similarly, the increment in equilibrium constant for bivalent diabody was greatest for the lowest affinity scFv C6G98A (65-fold) and least for the highest affinity scFv (7.7-fold).

To determine whether the magnitude of the decrease in K_D for diabody binding to cells was comparable with that observed for other bivalent antibody molecules, the affinity of a C6.5-Fc fusion protein was measured (20). In this recombinant antibody molecule, the C6.5 scFv was genetically linked to the hinge, C_H2, and C_H3 domains of human IgG1. The hinge region should allow similar flexibility to the scFv-binding sites as in an IgG antibody. The scFv-Fc fusion retains the intrinsic affinity of the parental scFv (20). The affinity of the bivalent C6.5-Fc fusion for binding to cells was determined (Fig. 2*D*) and is similar to that of the C6.5 diabody (3.9 nM *versus* 3.4 nM, respectively). The results indicate that differences in binding site flexibility and size of the molecules for these two bivalent molecules does not significantly affect the affinity for binding to cell surface antigens. This result also suggests that the relationship observed between monovalent and bivalent equilibrium constants observed for diabodies is likely to hold for other bivalent antibody constructs.

Biodistribution of Diabodies in *scid* Mice Bearing ErbB2-overexpressing Tumors. The relevance of the *in vitro* observations to *in vivo* tumor targeting was determined by measuring the biodistribution of the three diabodies and the C6.5 scFv in *scid* mice bearing s.c. SKOV3 tumors overexpressing the ErbB2 antigen. The tumor, blood, and organ retention of radioiodinated scFv and diabody molecules were determined at 1, 4, 24, 48, and 72 h after i.v. administration. As expected, the larger size (50 kDa) of the diabody constructs resulted in a prolonged blood retention as compared with that seen with the smaller (25 kDa) C6.5 scFv molecule (Fig. 3, *B*, *C*, and *D versus A*). This is reflected in the 4–5-fold greater blood AUC values for the diabody molecules as compared with C6.5 scFv (Table 4). The calculated $t_{1/2}\ \alpha$ for C6.5 scFv and diabody were 0.23 h and 0.67 h; the calculated $t_{1/2}\ \beta$ were 5.70 and 6.42 h, respectively. Diabodies exhibited significantly greater (2–5-fold) quantitative tumor retention at 24 h than was achieved with the highest affinity scFv studied (Fig. 3 and Table 4). This likely results from a combination of a higher apparent affinity, because of bivalent binding, and a slower serum clearance. Calculations of the cumulative residence of the radioiodinated diabodies and scFv, expressed as AUC, were determined. These were also significantly greater for diabodies compared with scFv (Table 4). Importantly, the difference in apparent affinity between diabodies did not significantly alter the quantitative tumor retention or tumor:blood ratios. In fact, the tumor AUC, tumor:blood AUC, and

Table 3 *Comparison of equilibrium constants of scFv and diabodies for binding to cells*

K_D values for binding to cells were determined by fitting the data from Fig. 2 to the Lineweaver-Burk equation.

Antibody	scFv K_D $[10^{-9}$ M]	Diabody K_D $[10^{-9}$ M]	K_D (scFv)/ K_D (diabody)
C6G98A	361	5.6	65
C6.5	70	3.4	18
C6ML3–9	3.8	0.49	7.7

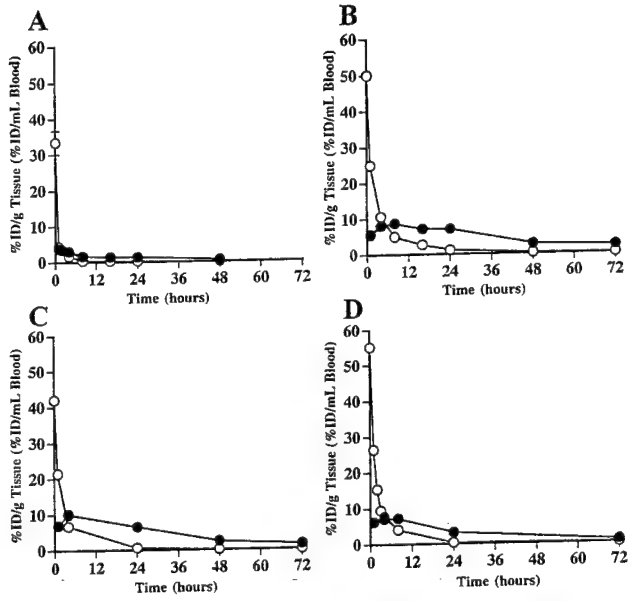

Fig. 3. The *in vivo* tumor targeting of radioiodinated scFv and diabodies. ScFv or diabody biodistribution studies were performed in SK-OV-3 tumor-bearing *scid* mice. Twenty micrograms of radioiodinated diabody or scFv were administered by i.v. tail vein injection to each mouse. Cohorts of five mice that received the ^{125}I-diabodies or scFv were sacrificed at the indicated time after injection. The plotted values represent the mean tumor (●) and blood (○) obtained from five mice per data point. *Bars* represent the SE. *A*, C6.5 scFv; *B*, C6G98A diabody; *C*, C6.5 diabody; *D*, C6ML3–9 diabody.

the 24-h tumor retention of the two lower-affinity diabodies (C6G98A and C6.5) were ~2-fold better than for the high-affinity C6ML39 diabody.

To determine whether the observed differences in AUC resulted from instability of the constructs, the diabodies were incubated in human serum for 3 days at 37°C and binding activities were compared by SPR. This study revealed that the constructs were very stable, with observed binding activities equal to 97% (C6G98A), 94% (C6.5), and 85% (C6ML3–9) of the original activity. This suggests that the observed differences in biodistribution reflect differences in the kinetic properties of the molecules, serum half-life, tumor penetration, and stability at the tumor site rather than proteolytic degradation in the circulation.

DISCUSSION

Bivalent and multivalent antibody-based molecules have recently been demonstrated to exhibit superior tumor retention properties as compared with monovalent fragments (5, 8, 11, 16, 24). Multiple approaches have been used in the construction of this class of molecules. These approaches range from direct cross-linking via a cysteine engineered onto the COOH-terminal of scFv (5) to the use of amphipathic helices to multimerize the scFv (10). However, the simplest approach takes advantage of scFv tendency to spontaneously form noncovalent dimers or diabodies. Because diabodies have molecular weights of ~M_r 50,000, they are small enough to be rapidly eliminated from the circulation via first-pass renal clearance. Because diabody size and molecular structure is similar to Fab fragments, it is expected that diabodies will readily penetrate from blood vessels into solid tumors, as reported for Fabs (6). The divalent nature of the interaction of diabodies with cell surface tumor antigen is widely recognized as being important in maintaining prolonged residence in tumors. What has been less clear is the precise relationship between the intrinsic affinity of the binding site, the increase in apparent affinity due to bivalent binding, and the impact of higher-affinity binding on *in vivo* tumor targeting.

The studies presented here were designed to examine the effect of affinity of a series of bivalent diabodies on their antigen-binding kinetics and their *in vitro* and *in vivo* tumor-targeting properties. Because all of the constructs were the same size and recognized the same epitope of ErbB2, any observed differences likely resulted solely from the differences in binding affinity. The role of valency on the impact of affinity was readily apparent when we compared the scFv and diabody constructs. The C6.5 scFv and its affinity mutants differ from each other by only one to three amino acid residues, yet differ in affinity for the same epitope of ErbB2 by 133-fold (18). However, when diabodies were constructed from the scFv, the resulting difference in affinity was reduced to only 22-fold. Most importantly, the greatest increment in affinity was observed for the diabody constructed from the lowest affinity scFv. Clearly, the kinetics of interaction is dependent on more than the straightforward additive impact of the individual affinities of the binding sites.

The equilibrium between a bivalent antibody and its antigen has often been depicted as a two-step reaction, involving free antibody and antigen as well as antibody, monovalently or bivalently complexed to its antigen. In this model, the association occurs in two steps. In the first reaction, the antibody monovalently binds to a single antigen before encountering a second antigen, after which the interaction can become bivalent. Whereas the rate of first reaction is determined by the association rate constant of the monovalent antibody arm, the second rate is dependent on external factors such as the density and fluidity of the antigen in the cell membrane (25) and the radius spanned by the antibody. In theoretical models of antibody interactions with cell surface antigen, it is often assumed that the antigen is in excess and the rate of bivalent binding solely depends on antigen diffusion (25, 26). In clinical use, however, large doses of antibody are used, potentially resulting in an excess of antibody at the binding site and the possibility of significant quantities of antigen bound monovalently.

To understand the dynamics of the binding kinetics, we studied the time dependence of bivalent binding of diabodies to ErbB2 by SPR under the conditions of high diabody concentration that might be expected in regions of tumor proximal to blood vessel. The results indicated that a large fraction of diabodies initially bind to only one antigen. Under these conditions, the bivalent dissociation rate constant decreased with increased binding time and the decrease in dissociation rate constant was inversely proportional to that of the monovalent interaction. Whereas the dissociation rate of the diabody with the lowest affinity rapidly stabilized at a 15-fold lower rate after 2 h of association, the decrease in the bivalent dissociation rate constant for the C6ML3–9 diabody was only 3-fold. One possible explanation for this result is that diabodies with lower intrinsic equilibrium constant can more rapidly achieve bivalent binding, because those bound monovalently dissociate rapidly freeing up antigen for bivalent bind-

Table 4 *Evaluation of targeting of 125I-labeled diabodies and scFv in tumor-bearing scid mice*

AUCs were calculated from the data in Fig. 3.

Antibody	Tumor AUC (% h^{-1} g^{-1})	Blood AUC (% h^{-1} ml^{-1})	Tumor: blood AUC	Calculated tumor:marrow AUC	24-h %ID/g tumor
scFv					
C6G98AscFv			ND[a]	ND	0.19
C6.5scFv	81.6	34.1	2.4:1	9.6:1	1.32
C6ML3–9scFv			ND	ND	1.42
Diabody					
C6G98Adb	433.0	178.9	2.4:1	9.6:1	7.07 ± 0.89[b]
C6.5db	405.1	132.7	3.0:1	12:1	6.48 ± 0.77
C6ML3–9db	259.1	140.5	1.8:1	7.2:1	3.18 ± 0.52

[a] ND, not determined.
[b] For the diabodies the SEs of the mean for the 24 h %ID are indicated.

ing by neighboring diabodies. Diabodies with higher intrinsic equilibrium constants dissociate more slowly from antigen and, thus, can prevent bivalent binding of neighboring diabodies. This effect has not been previously taken into account in theoretical models of bivalent binding.

The actual dynamics of the interaction between antibody and cell surface antigens in the tumor is, however, much more complex. The ability of IgG to extravasate and penetrate into tumor is severely limited by both the size of the antibody and the high hydrostatic pressure in the tumor resulting from a lack of draining lymphatics (27). This results in a very uneven distribution of the antibody, ranging from a situation of antibody excess in areas adjacent to the blood vessels to antigen excess in regions distant from the vasculature. Despite their improved tumor penetration properties, similar gradients will probably result from the administration of smaller scFv and diabody molecules (6).

In our study, the 22-fold difference in affinity (as determined by SPR) between the three diabodies did not result in greater quantitative tumor retention or tumor:blood ratio. In fact, the diabody constructed from the lowest affinity scFv (C6G98A) exhibited comparable tumor targeting to the diabody constructed from the higher-affinity C6.5 scFv and better targeting than the diabody constructed from the highest affinity C6ML3–9 scFv. Interestingly, the C6G98A scFv does not target tumor better than an irrelevant control scFv (9). We conclude that above a threshold affinity, other factors determine the quantitative tumor delivery of a bivalent antibody fragment. This is consistent with *in vivo* targeting results observed for the three C6.5-based scFv (9). This threshold affinity may be partly attributed to tumor physiology rather than simple antigen-binding kinetics. Indeed, barriers other than the antibody fragment size may exist in tumor tissue that restrict their penetration to areas distal from the blood vessels. Fujimori *et al.* (28) have postulated that high-affinity antibodies will not successfully penetrate deeply into tumors due to a binding site barrier effect, in which interaction with the first antigen encountered at the periphery of the tumor will block further diffusion of the antibody into the tumor. We have investigated the tumor penetration of the monovalent scFv used in this study. Whereas increasing the affinity improves the selective targeting of scFv to solid tumors (9) histochemical staining for scFv in the tumor xenografts supports the theory of Fujimori *et al.* (28).[4] This may explain why the C6ML3–9 diabody had significantly worse tumor-targeting properties than the other two diabodies.

In tumor-bearing immunodeficient mice, the 24-h tumor retentions of all three diabodies were superior to that of the highest affinity scFv. The differences in biodistributions of the diabodies and the scFv, thus, cannot be solely attributed to their K_D. This is apparent when comparing the tumor retention at 24 h of the C6G98A diabody to that of the higher-affinity C6ML3–9 scFv (7.1 *versus* 1.4%ID/g tumor and K_D = 5.6 nM *versus* 3.8 nM for the C6G98A diabody and C6ML3–9 scFv, respectively, for binding to cells). Clearly, the longer blood retention of the larger diabody molecules may account for some of the increased tumor retention because the diabodies would be expected to have more opportunities to perfuse the tumor and interact with target antigen. In addition, quantitative tumor localization may be affected by differences between kinetic *versus* equilibrium control of binding. The C6G98A diabody, with each binding site having a rapid dissociation rate constant, may be able to more easily dissociate from antigen and percolate through the tumor compared with a high-affinity scFv where the (single) binding site has a slower dissociation rate constant.

Differential effects of antibody fragment size, binding rates, and equilibrium constant on tumor penetration may explain the differences between our results and those of Viti *et al.* (29). In those studies, biodistributions of low-affinity (K_D = 41 nM) and high-affinity (K_D = 0.054 nM) scFv and their diabody dimers were studied in xenografted mice whose tumors expressed the neovascular antigen fibronectin. In contrast to our results, the higher-affinity scFv exhibited greater tumor retention than the diabody constructed from the lower-affinity scFv (4-fold higher %ID/g tumor at 24 h). In their model, tumor penetration is not an issue because the antigen is in the vasculature, whereas we studied an epithelial antigen where penetration will have a dramatic effect on antibody localization. A strict comparison of results between the two systems is not possible because: (*a*) Viti *et al.* (29) did not measure the apparent affinities of the diabodies; and (*b*) the "diabodies" had normal length linkers and, thus, could reequilibrate to mixtures of monomer and dimer after gel filtration and before injection into mice.

On the basis of our results, it is apparent that the construction of bivalent diabodies, even from low-affinity scFv, can lead to the generation of tumor-targeting agents that are superior to those achieved through the cumbersome processes involved in affinity maturing monovalent scFv molecules. This observation may have a significant impact on the design of future multivalent antibody-based molecules for cancer therapy.

REFERENCES

1. Huston, J. S., Levinson, D., Mudgett-Hunter, M., Tai, M. S., Novotny, J., Margolies, M. N., Ridge, R. J., Bruccoleri, R. E., Haber, E., Crea, R., and Oppermann, H. Protein engineering of antibody binding sites: recovery of specific activity in an anti-digoxin single-chain Fv analogue produced in *Escherichia coli*. Proc. Natl. Acad. Sci. USA, *85:* 5879–5883, 1988.
2. Bird, R. E., Hardman, K. D., Jacobson, J. W., Johnson, S., Kaufman, B. M., Lee, S. M., Lee, T., Pope, S. H., Riordan, G. S., and Whitlow, M. Single-chain antigen-binding proteins. Science (Washington DC), *242:* 423–426, 1988.
3. Begent, R. H., Verhaar, M. J., Chester, K. A., Casey, J. L., Green, A. J., Napier, M. P., Hope-Stone, L. D., Cushen, N., Keep, P. A., Johnson, C. J., Hawkins, R. E., Hilson, A. J., and Robson, L. Clinical evidence of efficient tumor targeting based on single-chain Fv antibody selected from a combinatorial library. Nat. Med., *2:* 979–984, 1996.
4. Colcher, D., Bird, R., Roselli, M., Hardman, K. D., Johnson, S., Pope, S., Dodd, S. W., Pantoliano, M. W., Milenic, D. E., and Schlom, J. *In vivo* tumor targeting of a recombinant single-chain antigen-binding protein. J. Natl. Cancer Inst., *82:* 1191–1197, 1990.
5. Adams, G. P., McCartney, J. E., Tai, M. S., Oppermann, H., Huston, J. S., Stafford, W. F. d., Bookman, M. A., Fand, I., Houston, L. L., and Weiner, L. M. Highly specific *in vivo* tumor targeting by monovalent and divalent forms of 741F8 anti-c-erbB-2 single-chain Fv. Cancer Res., *53:* 4026–4034, 1993.
6. Yokota, T., Milenic, D. E., Whitlow, M., and Schlom, J. Rapid tumor penetration of a single-chain Fv and comparison with other immunoglobulin forms. Cancer Res., *52:* 3402–3408, 1992.
7. Colcher, D., Pavlinkova, G., Beresford, G., Booth, B. J., Choudhury, A., and Batra, S. K. Pharmacokinetics and biodistribution of genetically-engineered antibodies. Q. J. Nucl. Med., *42:* 225–241, 1998.
8. Milenic, D. E., Yokota, T., Filpula, D. R., Finkelman, M. A., Dodd, S. W., Wood, J. F., Whitlow, M., Snoy, P., and Schlom, J. Construction, binding properties, metabolism, and tumor targeting of a single-chain Fv derived from the pancarcinoma monoclonal antibody CC49. Cancer Res., *51:* 6363–6371, 1991.
9. Adams, G. P., Schier, R., Marshall, K., Wolf, E. J., McCall, A. M., Marks, J. D., and Weiner, L. M. Increased affinity leads to improved selective tumor delivery of single-chain Fv antibodies. Cancer Res., *58:* 485–490, 1998.
10. Pack, P., and Plückthun, A. Miniantibodies: use of amphipathic helices to produce functional, flexibly linked dimeric FV fragments with high avidity in *Escherichia coli*. Biochemistry, *31:* 1579–1584, 1992.
11. Hu, S., Shively, L., Raubitschek, A., Sherman, M., Williams, L. E., Wong, J. Y., Shively, J. E., and Wu, A. M. Minibody: a novel engineered anti-carcinoembryonic antigen antibody fragment (single-chain Fv-CH3) which exhibits rapid, high-level targeting of xenografts. Cancer Res., *56:* 3055–3061, 1996.
12. Wu, A. M., Chen, W., Raubitschek, A., Williams, L. E., Neumaier, M., Fischer, R., Hu, S. Z., Odom-Maryon, T., Wong, J. Y., and Shively, J. E. Tumor localization of anti-CEA single-chain Fvs: improved targeting by non-covalent dimers. Immunotechnology, *2:* 21–36, 1996.
13. Whitlow, M., Filpula, D., Rollence, M. L., Feng, S. L., and Wood, J. F. Multivalent Fvs: characterization of single-chain Fv oligomers and preparation of a bispecific Fv. Protein Eng., *7:* 1017–1026, 1994.
14. Holliger, P., Prospero, T., and Winter, G. Diabodies: small bivalent and bispecific antibody fragments. Proc. Natl. Acad. Sci. USA, *90:* 6444–6448, 1993.

[4] G. P. Adams, R. Schier, A. M. McCall, H. Simmons, E. M. Horak, R. K. Alpaugh, J. D. Marks, and L. M. Weiner. High affinity restricts the localization and tumor penetration of single chain Fv antibody molecules, submitted for publication.

15. Perisic, O., Webb, P. A., Holliger, P., Winter, G., and Williams, R. L. Crystal structure of a diabody, a bivalent antibody fragment. Structure, *2:* 1217–1226, 1994.
16. Adams, G. P., Schier, R., McCall, A. M., Crawford, R. S., Wolf, E. J., Weiner, L. M., and Marks, J. D. Prolonged *in vivo* tumour retention of a human diabody targeting the extracellular domain of human HER2/neu. Br. J. Cancer, *77:* 1405–1412, 1998.
17. Schier, R., Marks, J. D., Wolf, E. J., Apell, G., Wong, C., McCartney, J. E., Bookman, M. A., Huston, J. S., Houston, L. L., Weiner, L. M., and Adams, G. P. *In vitro* and *in vivo* characterization of a human anti-c-erbB-2 single-chain Fv isolated from a filamentous phage antibody library. Immunotechnology, *1:* 73–81, 1995.
18. Schier, R., McCall, A., Adams, G. P., Marshall, K. W., Merritt, H., Yim, M., Crawford, R. S., Weiner, L. M., Marks, C., and Marks, J. D. Isolation of picomolar affinity anti-c-erbB-2 single-chain Fv by molecular evolution of the complementarity determining regions in the center of the antibody binding site. J. Mol. Biol., *263:* 551–567, 1996.
19. Pinilla, C., Buencamino, J., Appel, J. R., Hopp, T. P., and Houghten, R. A. Mapping the detailed specificity of a calcium-dependent monoclonal antibody through the use of soluble positional scanning combinatorial libraries: identification of potent calcium-independent antigens. Mol. Divers., *1:* 21–28, 1995.
20. Powers, D. B., Amersdorfer, P., Poul, M. A., Nielsen, U. B., Shalaby, M. R., Adams, G. P., Weiner, L. M., and Marks, J. D. Expression of single-chain Fv-Fc fusions in *Pichia pastoris*. J. Immunol. Methods, in press, 2000.
21. Benedict, C. A., MacKrell, A. J., and Anderson, W. F. Determination of the binding affinity of an anti-CD34 single-chain antibody using a novel, flow cytometry based assay. J. Immunol. Methods, *201:* 223–231, 1997.
22. Laub, P. B., and Gallo, J. M. NCOMP—a windows-based computer program for noncompartmental analysis of pharmacokinetic data. J. Pharm. Sci., *85:* 393–395, 1996.
23. DeNardo, S. J., Mirick, G. R., Kroger, L. A., O'Grady, L. F., Erickson, K. L., Yuan, A., Lamborn, K. R., Hellstrom, I., Hellstrom, K. E., and DeNardo, G. L. The biologic window for chimeric L6 radioimmunotherapy. Cancer (Phila.), *73:* 1023–1032, 1994.
24. Pavlinkova, G., Beresford, G. W., Booth, B. J., Batra, S. K., and Colcher, D. Pharmacokinetics and biodistribution of engineered single-chain antibody constructs of MAb CC49 in colon carcinoma xenografts. J. Nucl. Med., *40:* 1536–1546, 1999.
25. Kaufman, E. N., and Jain, R. K. Effect of bivalent interaction upon apparent antibody affinity: experimental confirmation of theory using fluorescence photobleaching and implications for antibody binding assays. Cancer Res., *52:* 4157–4167, 1992.
26. Crothers, D. M., and Metzger, H. The influence of polyvalency on the binding properties of antibodies. Immunochemistry, *9:* 341–357, 1972.
27. Jain, R. K. Physiological barriers to delivery of monoclonal antibodies and other macromolecules in tumors. Cancer Res., *50:* 814s–819s, 1990.
28. Fujimori, K., Covell, D. G., Fletcher, J. E., and Weinstein, J. N. Modeling analysis of the global and microscopic distribution of immunoglobulin G, F(ab')2, and Fab in tumors. Cancer Res., *49:* 5656–5663, 1989.
29. Viti, F., Tarli, L., Giovannoni, L., Zardi, L., and Neri, D. Increased binding affinity and valence of recombinant antibody fragments lead to improved targeting of tumoral angiogenesis. Cancer Res., *59:* 347–352, 1999.

Nuclear Medicine & Biology, Vol. 27, pp. 339–346, 2000

ISSN 0969-8051/00/$–see front matter
PII S0969-8051(00)00103-7

Delivery of the α-Emitting Radioisotope Bismuth-213 to Solid Tumors via Single-Chain Fv and Diabody Molecules

G. P. Adams,[1] C. C. Shaller,[1] L. L. Chappell,[2] C. Wu,[2] E. M. Horak,[1] H. H. Simmons,[1] S. Litwin,[1] J. D. Marks,[3] L. M. Weiner[1] and M. W. Brechbiel[2]

[1]DEPARTMENT OF MEDICAL ONCOLOGY, FOX CHASE CANCER CENTER, PHILADELPHIA, PENNSYLVANIA USA; [2]NATIONAL CANCER INSTITUTE, NATIONAL INSTITUTES OF HEALTH, BETHESDA, MARYLAND USA; AND [3]DEPARTMENT OF ANESTHESIOLOGY AND PHARMACEUTICAL CHEMISTRY, UNIVERSITY OF CALIFORNIA AT SAN FRANCISCO, SAN FRANCISCO, CALIFORNIA USA

ABSTRACT. Intravenously administered anti-tumor single-chain Fv (scFv) and diabody molecules exhibit rapid clearance kinetics and accumulation in tumors that express their cognate antigen. In an attempt to fit the rate of isotope decay to the timing of delivery and duration of tumor retention, anti-HER2/*neu* CHX-A″ DTPA-C6.5K-A scFv and diabody conjugates were labeled with the α-particle emitter ^{213}Bi ($t_{1/2}$ = 47 min). Radioimmunotherapy studies employing 0.64, 0.35, or 0.15 μCi of ^{213}Bi-labeled C6.5K-A diabody or 1.1, 0.6, or 0.3 μCi of ^{213}Bi-labeled C6.5K-A scFv were performed in nude mice bearing early, established SK-OV-3 tumors. Only the 0.3 μCi dose of ^{213}Bi-labeled C6.5K-A scFv resulted in both acceptable toxicity and a reduction in tumor growth rate. The specificity of the anti-tumor effects was determined by comparing the efficacy of treatment with 0.3 and 0.15 μCi doses of ^{213}Bi-labeled C6.5K-A scFv and ^{213}Bi-labeled NM3E2 (an irrelevant scFv) in nude mice bearing large established tumors. The 0.3 μCi dose of ^{213}Bi on both the C6.5K-A and NM3E2 scFvs resulted in similar anti-tumor effects (p = 0.46) indicating that antigen-specific targeting was not a factor. This suggests that the physical half-life of ^{213}Bi may be too brief to be effectively paired with systemically-administered diabody or scFv molecules. NUCL MED BIOL 27;4: 339–346, 2000. © 2000 Elsevier Science Inc. All rights reserved.

KEY WORDS. α Particles, Single-chain Fv, Diabody, Radioimmunotherapy, Solid tumors

INTRODUCTION

The field of radioimmunotherapy (RAIT) has been recently buoyed by reports of successes in the treatment of hematologic malignancies with ^{131}I-labeled (17, 29) and ^{90}Y-labeled (19) monoclonal antibodies (MAb). Although sporadic reports of success exist for RAIT of solid tumors (5), these rates are far below those achieved in diffuse malignancies. This is largely due to the physiology of solid tumors. Unlike normal tissues, tumors lack draining lymphatics and consistently outgrow their blood supply (15, 16). As a result, high hydrostatic pressures develop inside the tumor, which in turn limit the diffusion of large macromolecules (e.g., intact immunoglobulin G [IgG]) into the tumor microenvironment.

In an attempt to circumvent these impediments, application of smaller engineered antibody-based proteins has been developed. The 25-kDa single-chain Fv (scFv) and the 50-kDa diabody are two such molecules. The scFv is composed of the variable light and variable heavy chains of an IgG molecule joined by a 15 amino acid spacer that holds the two chains together and allows them to form a single binding pocket (14). In contrast, the diabody is a scFv dimer formed by shortening the spacer between the light and heavy chains from 15 to 5 amino acids, thereby preventing the chains from a single molecule from associating to form a binding pocket (13). Because the light and heavy chains have a high affinity for each other, the light chain from one molecule associates with the heavy chain of a second (and vice versa), leading to the production of a noncovalent dimer.

Small engineered scFv and diabody molecules are rapidly cleared from the circulation of immunodeficent mice, leading to highly specific tumor retention of minimal quantities of radionuclide in the terminal phases of their distribution (2, 3, 8, 24, 35, 36). However, their small sizes also allow for a rapid delivery to tumor and mediate effective tumor penetration. Because these final two properties are highly desirable in the selection of effective agents for the RAIT of solid tumors, the challenge remains to pair these molecules with isotopes that are well matched to rapid transit to tumor and relatively transient tumor retention. In mice, the majority of the tumor residence occurs within the first 12 h after injection for the scFv and within the first 24 h after injection for the diabody. Because the classical RAIT isotope ^{131}I has a half-life of 192 h, ^{131}I conjugated to a scFv or diabody will likely undergo most of its disintegrations long after the radioimmunoconjugate has cleared from the tumor and has been eliminated from the host. Similarly, the shorter-lived isotope ^{90}Y ($t_{1/2}$ = 64 h) may still have too long a physical half-life to be effective in this setting. In a study describing the potential of anti-CEA diabodies to serve as vehicles for the delivery of short-lived isotopes for RAID, Wu *et al.* (36) reported optimal planar imaging of human tumor xenografts in athymic mice at 6 h and the ability to detect the tumors as early as 2 h after administration of ^{123}I-labeled diabody (physical $t_{1/2}$ = 13.2 h). In the same study, it was calculated that the optimal time for positron emission tomography (PET) imaging with ^{18}F-labeled

Supported by National Cancer Institute Grant CA65559, Department of Defense Grant DAMD17-98-1-8307, the Bernard A. and Rebecca S. Bernard Foundation, the Frank Strick Foundation, and an appropriation from the Commonwealth of Pennsylvania.

Address correspondence to: G. P. Adams, Ph.D., Department of Medical Oncology, Fox Chase Cancer Center, 7701 Burholme Ave., Philadelphia, PA 19111; e-mail: gp_adams@fccc.edu.

Received 1 March 2000.
Accepted 21 March 2000.

diabody (physical $t_{1/2}$ = 110 min) would occur 1.4 h after administration.

The use of the α emitters, namely ^{212}Bi, ^{213}Bi, and ^{211}At, have recently attracted attention for their potential use in RAIT. In particular, ^{213}Bi ($t_{1/2}$ = 47 min) has been proposed as a viable candidate due to a combination of availability and the lack of a requirement for specialized production and labeling facilities. In addition, it has been proposed that successful RAIT will result from the matching of half-lives of the isotope and the delivery vector (10, 11). Finally, the track length of α particles is significantly shorter than that of β particles (22). Therefore, when employed for RAIT, the cytotoxicity should be more focused at tumor sites with less potential for collateral damage of normal tissue.

In the current study we have conjugated the anti-HER2/*neu* C6.5K-A scFv and diabody molecules to CHX-A″, a single enantiomer of 2-(*p*-isothiocyanatobenzyl)-cyclohexyl-diethylenetriaminepentaacetic acid (CHX-DTPA), which is a recently developed backbone-substituted derivative of DTPA (38). Using these radioimmunoconjugates, we have begun to determine the conditions that may lead to the most favorable pairing of isotopes with the new generation of engineered antibody fragments.

MATERIALS AND METHODS

The C6.5K-A scFv (C6.5K100gA) and diabody molecules differ from the native C6.5 sequence by a single amino acid substitution in the heavy chain CDR3 (30, 31). This format was employed because the original C6.5 molecule has a lysine in the heavy chain CDR3 that prohibits use of chelate conjugation strategies that target amino groups. The C6.5K-A and C6.5 scFv molecules both have similar affinities (31) and biodistributions when labeled with ^{125}I by the chloramine T method (data not shown). Both molecules were produced by periplasmic expression from *Escherichia coli* in shake flasks and purified by immobilized metal affinity chromatography (IMAC) and subsequent size exclusion chromatography as previously described (30, 31).

Conjugation

The bifunctional chelating agent CHX-A″ DTPA (38) was conjugated to the C6.5K-A scFv, the C6.5K-A diabody, and an irrelevant negative control scFv NM3E2 (specific for CD16) as previously described (25). The final antibody concentration was measured spectrophotomerically using an extinction coefficient of 1.4 mL/mg/cm for the scFv and diabody molecules, and the chelate to protein ratio was determined as described in the literature (28).

^{213}Bi-Labeling

^{213}Bi was selectively eluted from a generator that had been prepared with 20 μCi ^{225}actinium chloride ($^{225}AcCl_3$; Oak Ridge Natl. Laboratories, Oak Ridge, TN USA) as described in the literature (37). Briefly, two syringes containing 25 mL of metal-free water and one syringe containing 11 mL ultrapure 1.0 M HCl were placed on a syringe pump set at the rate of 1 mL/min. Tubing from all three syringes combined in an acrylic mixing chamber containing a magnetic stir bar. The effluent from the mixing chamber was then introduced into the generator, displacing the ^{213}Bi into an AG 50WX4 cation resin column. ^{213}Bi was eluted from the cation resin with 0.8 mL of 0.1 M HI. The eluted ^{213}Bi was neutralized to pH 5.0 by the addition of 40 μL of 5.0 M NaOAc and the radioisotope was incubated with 300–400 μg of CHX-A″ conjugated scFv or diabody for 10 min at room temperature. Ten microliters of 0.1 M ethylene diamine tetraacetic acid (EDTA) were added to chelate any unincorporated ^{213}Bi and the labeled proteins were purified by the centrifuged Sephadex G50-80 column method (23). The specific activity of the ^{213}Bi radiopharmaceuticals was determined using a dose calibrator (Capintech Model CRC-35R, Capintech Inc., Ramsey, NJ USA) set at the National Institute of Standards and Technology dictated setting of 38. The quality of the labeled scFv and diabody molecules was assessed by ITLC and in live cell binding assays (1). In the ITLC assays, 1 μL from each reaction mixture and final product was applied to silica ITLC strips (Biodex Medical Systems, Shirley, NY USA) and allowed to migrate using normal saline as a mobile phase. The strips were cut at the midpoint and the top and bottom halves were counted in a gamma well counter (Gamma4000, Beckman, Irvine, CA USA). The immunoreactivities of the radiopharmaceuticals were determined in a live cell binding assay (1). Briefly, 10 ng of labeled scFv or diabody in 100 μL phosphate-buffered saline (PBS) was added in triplicate into 15 mL polypropylene centrifuge tubes containing 5 × 10^6 SK-OV-3 human ovarian carcinoma cells (HTB 77; ATCC), which overexpress the HER2/*neu* antigen. The cells were allowed to incubate for 30 min at room temperature. Two milliliters of PBS were added to each tube and they were centrifuged for 5 min at 500 × g. Supernatants were separated from the cell pellets, both were transferred to 12 × 75 counting tubes and the percentage of radioactivity associated with the cell pellet was determined by counting in a gamma-counter.

Therapy Studies

SK-OV-3 cells were implanted subcutaneously in the abdomens of 8-week-old male athymic nude mice (Taconic Labs, Germantown, NY USA). The first therapy study was performed at 10 days following the implantation of 5 × 10^6 cells (mean tumor size = 68 ± 5 mm^3). To reduce the nontargeted renal and reticuloendothelial retention of the ^{213}Bi, each mouse was given 100 mg of L-lysine (Sigma Chemical Co., Cat. #L-6027, St. Louis, MO USA) in 250 μL of normal saline by intraperitoneal injection 2 h prior to initiating the therapy study. Cohorts of five mice were treated with ^{213}Bi-labeled CHX-A″-C6.5K-A diabody, ^{213}Bi-labeled CHX-A″-C6.5K-A scFv, or unlabeled C6.5K-A diabody or scFv. The mice treated with ^{213}Bi-labeled CHX-A″-C6.5K-A diabody received 640, 400, or 150 μCi (72, 48, and 16 μg, respectively). Mice treated with ^{213}Bi-labeled CHX-A″-C6.5K-A scFv received 1,100, 600, or 300 μCi (300, 196, and 102 μg, respectively). The tumors were measured with calipers and body weights were obtained two to three times weekly. The mice were also observed for signs of toxicity. Tumor volumes were determined using the ellipsoidal formula: length (mm) × width (mm) × height (mm) × 0.52 (derived from π/6) (12). The study was terminated when tumor volumes exceeded 10% of the animal's body weight.

A second therapy study was performed to determine if the tumor growth inhibition observed with ^{213}Bi-labeled CHX-A″-C6.5K-A scFv treatment in the initial study was specific in nature. In this case, mice bearing established SK-OV-3 tumors (mean tumor size = 16.6 ± 8.1 mm^3) were employed 30 days after the subcutaneous implantation of 2.5 × 10^6 cells. Cohorts of mice were treated with a single intravenous injection of ^{213}Bi-labeled CHX-A″ conjugated to either the C6.5K-A scFv (10 mice per treatment group) or the NM3E2 scFv (5–6 mice per treatment group), which is specific for CD16 antigen that is not expressed in the mouse. Treatment doses were 300 μCi (166–340 μg) or 150 μCi (83–110 μg) of ^{213}Bi-

labeled CHX-A″ conjugated to either scFv. Control mice were treated with 80 μg of unconjugated (cold) C6.5K-A scFv. Tumor measurements and animal weights were acquired every 3–4 days and tumor volumes were calculated as described above. The study was terminated when the mice became moribund or when their tumor volumes exceeded 10% of the animal's weight. The significance of the difference in growth rates of the tumors in the treatment and control groups was determined using Wilcoxon one-sided tests.

RESULTS

Antibodies

The C6.5K-A scFv and C6.5K-A diabody molecules employed in the first therapy study were determined to have an average of 0.55 and 0.48 CHX-A″ ligands associated per antibody molecule, respectively. The C6.5K-A scFv and NM3E2 scFv molecules employed in the second therapy study had 1.1 and 0.8 CHX-A″ ligands associated per antibody molecule, respectively. In the ITLC assays of the radiopharmaceuticals, it was determined that 97% (C6.5K-A diabody), 96% (C6.5K-A scFv, first study), 98% (C6.5K-A scFv, second study), and 97% (NM3E2 scFv) of the activity did not migrate and thus was protein associated. The average immunoreactivities were well within the customary range for each anti-HER2/*neu* molecule, with values of 57% and 64%, respectively, for the C6.5K-A scFv and diabody molecules and less than 2% for the NM3E2 scFv negative control.

Therapy Studies

The initial therapy study was performed to determine the maximum tolerated dose (MTD) of ^{213}Bi-labeled CHX-A″-C6.5K-A scFv and diabody molecules and to acquire preliminary evidence of the efficacy of utilizing these conjugated α emitters for the treatment of solid tumors. To assess the MTD, weight measurements of the treated mice were acquired two to three times per week and they were observed for outward signs of toxicity. The mice treated with the 640 μCi and 400 μCi doses of ^{213}Bi-labeled CHX-A″-C6.5K-A diabody exhibited marked decreases in body weight (29 ± 7%) within 6 days following receipt of treatment. By day 7, all of the 640 μCi group and two of the five mice in the 400 μCi group had died (Fig. 1B). Although the mice that received the 150 μCi dose of ^{213}Bi-labeled CHX-A″-C6.5K-A diabody did not exhibit a similar weight loss, the dose was still lethal in two of the five treated animals. Similar toxicities were observed with the ^{213}Bi-labeled CHX-A″-C6.5K-A scFv. However, its faster equilibration and elimination phases in circulation were associated with a higher MTD for ^{213}Bi. This was demonstrated by the survival of all of the animals that received the 300 μCi dose (Fig. 1A). However, the dose was still toxic, as evidenced by an average weight loss of 10% by the tenth day after the treatment. As above with the diabody, the greatest toxicity was observed in the two higher dose groups. Both 1,100 μCi and 600 μCi doses of ^{213}Bi-labeled CHX-A″-C6.5K-A scFv were completely lethal (Fig. 1A).

The therapeutic efficacies of treatment at the best-tolerated doses in the first study are displayed in Figure 2. In this experiment, the 300 μCi of ^{213}Bi-labeled CHX-A″-conjugated C6.5K-A scFv led to an approximately 2-week delay in the doubling time of the early subcutaneous SK-OV-3 tumors compared with that observed in the untreated control group (34 days versus 21 days, respectively; Fig. 2A). In contrast, a 150 μCi dose of ^{213}Bi-labeled CHX-A″-C6.5K-A diabody did not significantly alter the tumor growth rate from that observed in the untreated mice (Fig. 2B).

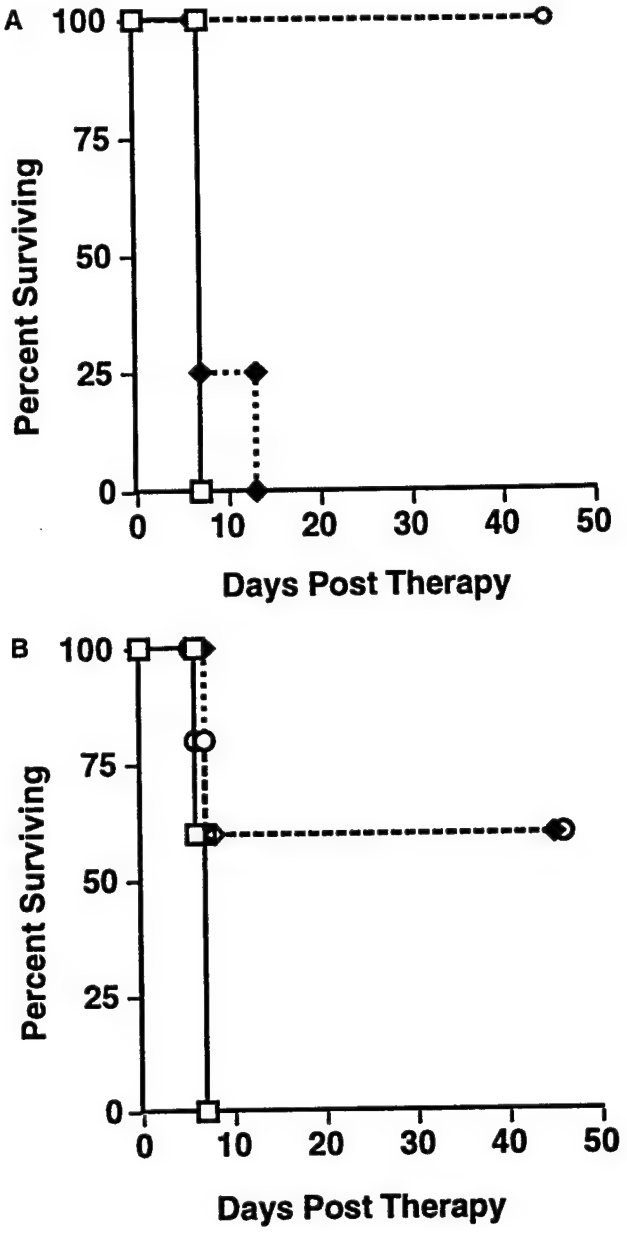

FIG. 1. Survival of SK-OV-3 tumor-bearing nude mice following therapy with ^{213}Bi-labeled CHX-A″-C6.5K-A single-chain Fv (scFv) or diabody. (A) Mice receiving 1.1 μCi (squares), 0.6 μCi (diamonds), or 0.3 μCi (circles) of ^{213}Bi-labeled CHX-A″-C6.5K-A scFv. (B) Mice receiving 0.64 μCi (squares), 0.4 μCi (diamonds), or 0.15 (circles) μCi of ^{213}Bi-labeled CHX-A″-C6.5K-A diabody. N = 5 mice per group.

Based on the above results, a second therapy study focused exclusively on ^{213}Bi-labeled scFv constructs. In this trial mice bearing established SK-OV-3 tumors (mean tumor size = 16.6 ± 8.1 mm^3) were treated with a single intravenous injection of ^{213}Bi-labeled CHX-A″ conjugated to either the anti-HER2/*neu* C6.5K-A scFv (10 mice per treatment group) or the irrelevant control NM3E2 scFv (5–6 mice per treatment group). Separate groups were treated with either 300 μCi (166–340 μg) or 150 μCi (83–110 μg) of ^{213}Bi-labeled CHX-A″ conjugated to each scFv.

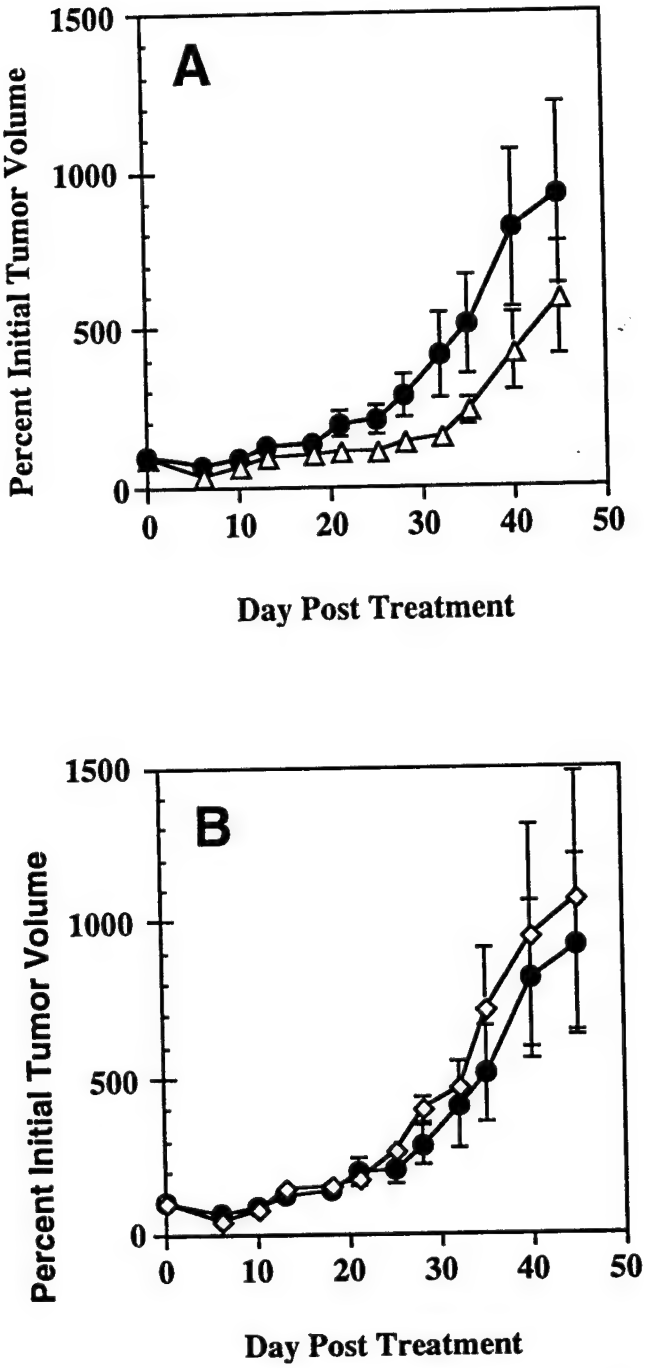

FIG. 2. ^{213}Bi-labeled CHX-A″-C6.5K-A diabody and single-chain Fv (scFv) therapy of early tumors. Nude mice with small palpable (10 days postimplantation) SK-OV-3 ovarian carcinoma tumors were treated with a single intravenous dose of (A) 0.15 μCi ^{213}Bi-labeled CHX-A″-C6.5K-A scFv (triangles) or (B) 0.30 μCi ^{213}Bi-labeled CHX-A″-C6.5K-A diabody (diamonds). Untreated control mice (circles) are included in each graph. Results are presented as the percent of initial tumor volume (mm^3). N = 5 mice per group. Two mice in the diabody treatment group died from treatment-related toxicity prior to day 7 following therapy. SEMs are indicated.

Control mice were treated with 80 μg of unconjugated (cold) C6.5K-A scFv. As evidenced by weight loss, only minimal treatment-associated toxicity was observed in this study (−3.4% and −9.9% for the 150 μCi and 300 μCi groups, respectively). A single 150 μCi dose of ^{213}Bi conjugated to either the C6.5K-A or NM3E2 scFvs did not significantly impact the rate of tumor growth compared with control mice treated with unlabeled C.5 scFv (p = 0.1124 and 0.5152; Fig. 3). Increasing the dose to 300 μCi of ^{213}Bi-labeled CHX-A″-C6.5K-A scFv resulted in a significantly decreased tumor growth rate compared with the controls treated with unlabeled C6.5K-A scFv (p = 0.0032; Fig. 3). However, because similar growth delays resulted from treatment with 300 μCi of ^{213}Bi using both the anti-Her2/*neu* and irrelevant scFv vehicles (p = 0.4624), the observed effects were not tumor-specific. The growth plots corresponding to individual tumors are provided in Figure 4.

DISCUSSION

Many major obstacles to the success of RAIT have been overcome. In particular, the field of chelation chemistry has provided new agents that have very high affinities for a variety of radiometals. One such molecule, CHX-A″ DTPA, was employed in this study. The CHX-A″ DTPA is a versatile chelator that has been shown to bind radiometals such as ^{111}In, ^{90}Y, and ^{212}Bi or ^{213}Bi with excellent stability and suitable formation kinetics to obviate radiolysis effects (20). This has allowed us to perform biodistribution studies with ^{111}In-CHX-A″-labeled scFv and diabody to predict tumor-specific distributions that would be achieved with the shorter-lived, and more difficult to track, α-emitter ^{213}Bi (data not shown).

The small size of scFv molecules leads to their rapid renal elimination. When these molecules are labeled with radioiodine, dehalogenation occurs and the iodine is excreted in the urine. However, a very different pattern of renal retention occurs when a radiometal is employed as a trace or therapeutic label on an scFv molecule. In a study comparing the metabolic patterns of ^{125}I and ^{177}Lu labeled scFv, Schott *et al.* (32) observed that significantly greater renal and reticuloendothelial retention was associated with the use of radiometals. Similar observations have been made by a number of groups when larger Fab fragments are employed in place of scFv molecules (9, 27).

Recently a number of groups have described the utility of employing doses of cationic amino acids to decrease the renal retention of radiolabeled antibody fragments (6, 7, 9, 27). Prior to initiating the current study, we evaluated the utility of using intraperitoneal injections of L-lysine to achieve similar results with ^{111}In-labeled CHX-A″-C6.5K-A diabody (data not shown). We did not achieve the five- to sixfold reduction in renal uptake that was observed by Behr *et al.* (6) when L-lysine was administered prior to ^{125}I-Fab′. However, we did observe significant decreases in renal retention in the presence of L-lysine without altering the tumor-targeting properties of the radiolabeled diabody. Accordingly, we decided to preadminister L-lysine in the therapy/MTD studies to reduce the potential for renal toxicity.

This is the first report of the use of α-emitting radioisotopes with engineered antibody fragments. α-Emitting radioisotopes have a number of properties that make them highly attractive for RAIT applications. These include a high linear energy transfer (LET) and a high relative biological effectiveness for cell kill stemming from the inability of cells to repair damage resulting from α-particle transversal (34). The therapeutic potential of α emitters is apparent when they are compared with commonly employed β emitters. One

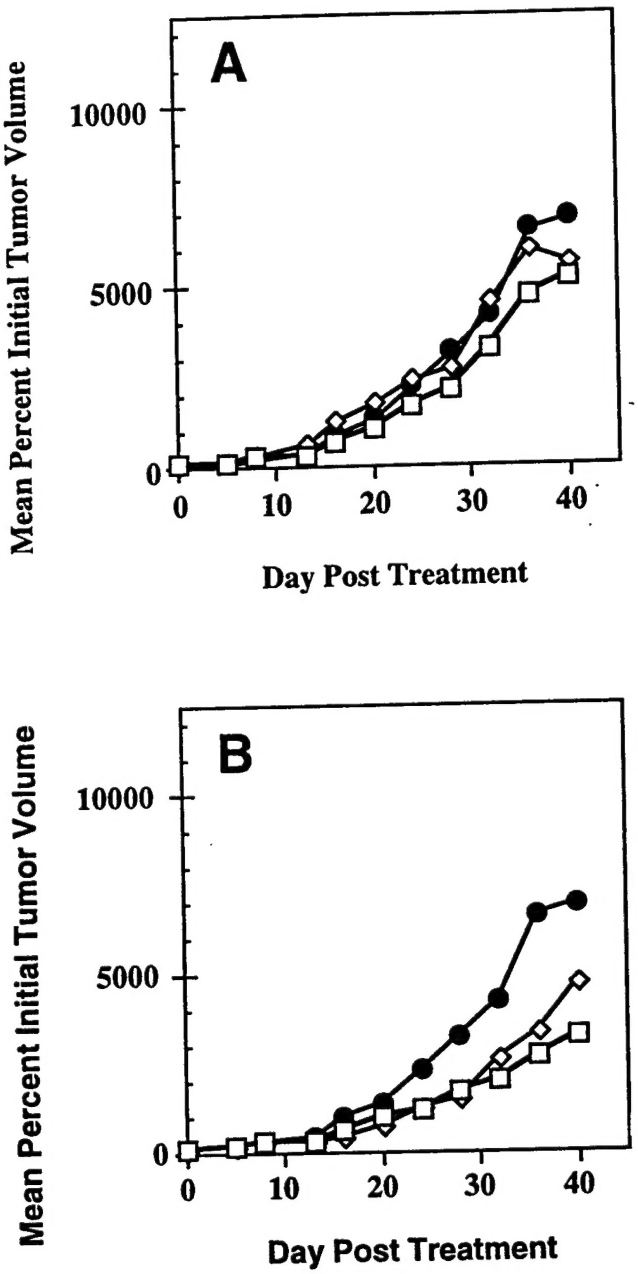

FIG. 3. ^{213}Bi-labeled CHX-A″-C6.5K-A single-chain Fv (scFv) therapy of established tumors. Nude mice bearing large (mean = 16.6 ± 18.1 mm^3) SK-OV-3 tumors were treated with (A) 0.15 μCi or (B) 0.3 μCi of ^{213}Bi conjugated to C6.5K-A scFv (squares) or to NM3E2 scFv (diamonds), an irrelevant control specific for CD16. Control mice treated with unlabeled C6.5K-A scFv (circles) are included in each graph. Results are presented as the mean percent of initial tumor volume (mm^3) for each group. N = 10 mice for all C6.5K-A groups and 6 and 5 mice, respectively, for the low- and high-dose NM3E2 groups. Graphs detailing individual mice are presented in Figure 4.

of the most promising β emitters employed in RAIT is ^{90}Y, which has a LET of 0.2 keV/μm and a mean range in tissue of approximately 4 mm. In contrast, the most attractive α emitters (^{211}At and ^{213}Bi) have an approximately 500-fold greater LET (approximately 100 keV/μm) and a 55-fold shorter mean range in tissue (70 μm) (22). When employed in targeted therapy, this translates into significantly greater specificity and efficiency of effect. Furthermore, unlike the situation with β particles, the presence of oxygen is not required for α-particle–based cell killing. Hence, they can be effective even in hypoxic regions of tumors. However, whereas β-emitting isotopes have been extensively employed in RAIT, α-emitting isotopes have largely been bypassed, primarily due to half-life imposed difficulties inherent in their production and shipping. The recent development of generators for the production of α emitters, such as the ^{225}Ac/^{213}Bi generator we employed here (37), has overcome the major hurdle to their use.

To date, short-lived α-emitter (e.g., ^{213}Bi, ^{212}Bi, or ^{211}At)-based RAIT has been most effective when employed in preclinical trials to treat tumors that are in a defined compartment, accessible through regional delivery of the radiopharmaceutical, or readily accessible from the circulation. Examples of regional approaches include the successful treatment of intraperitoneal EL-4 ascites tumors with ^{212}Bi-labeled IgM specific for Thy 1.2 by Macklis *et al.* (21) and the prolonged survival of mice bearing intraperitoneal LS174T colon carcinoma following treatment with ^{212}Bi-labeled B72.3 MAb (33). The potential of α-emitter–based RAIT of targets that are readily accessible to the circulation has been demonstrated in leukemia models in mice (22, 26) and in studies by Kennel and Mirzadeh (18) that targeted vascular cells to treat adjacent lung tumors. In the latter model, treatment of mice with ^{213}Bi-labeled MAb 201B, specific for murine thrombomodulin, extended the life span of mice bearing multiple small (50–400 cell) EMT-6 lung tumors. Accordingly, a major goal of the present study was to determine if the pairing of a short-lived α emitter with a rapidly localized (and cleared) targeting agent could extend the utility of this class of isotopes to the treatment of solid subcutaneous tumors.

The studies presented here indicate that ^{213}Bi can be conjugated successfully to the scFv and diabody molecules via the CHX-A″ chelate. Our preliminary preclinical therapy trials demonstrated that significant reductions in the growth rates of early and established human tumor xenografts could be achieved by treating the mice with 0.3 μCi of ^{213}Bi chelated to the anti-HER2/*neu* scFv C6.5K-A. However, we observed similar results when the ^{213}Bi was conjugated to an irrelevant control scFv, suggesting that the anti-tumor effects were nonspecific in nature. This is consistent with the observation that both scFv molecules display similar pharmacokinetics (data not shown) and with our previously published results that reported significant tumor localization of both anti-tumor and irrelevant scFv 1 h postinjection (2). Because both molecules had potentially similar early (nonspecific) tumor and vascular levels, it is not surprising that they displayed equal anti-tumor effects when combined with short-lived, short track-length isotopes. Alternatively, the lack of a tumor-specific therapeutic effect could result from instability of the scFv and diabody molecules *in vivo*. However, we believe this to be extremely unlikely because the *in vivo* tumor targeting properties of both molecules have been fully characterized in a similar model system using ^{125}I- (3, 4, 30) and ^{111}In-labeled CHX-A″ chelate-conjugation (unpublished data) strategies.

The ability of the α particles to penetrate tissues (70 μm average track length) is very short compared with the tumor radii (ranging from 5–8 mm and 2–3 mm in the first and second studies, respectively). Thus, it is likely that the observed decrease in tumor growth rate resulted from exposures received by tumor vasculature, neovasculature, and tumor cells in the immediate vicinity of the blood vessels. However, in light of the nonspecific nature of current chemotherapeutic drugs, an effective radiopharmaceutical with a

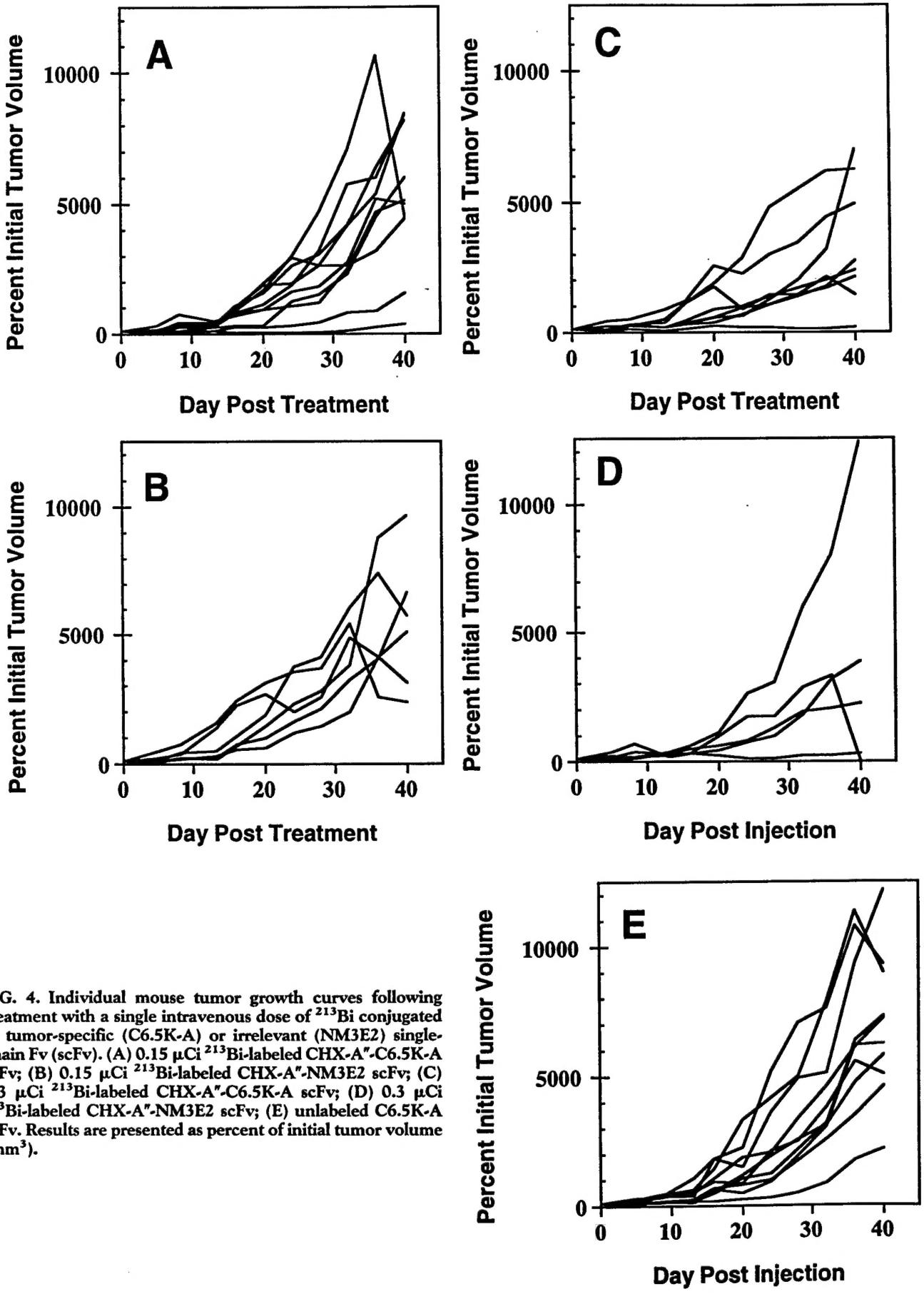

FIG. 4. Individual mouse tumor growth curves following treatment with a single intravenous dose of ^{213}Bi conjugated to tumor-specific (C6.5K-A) or irrelevant (NM3E2) single-chain Fv (scFv). (A) 0.15 μCi ^{213}Bi-labeled CHX-A″-C6.5K-A scFv; (B) 0.15 μCi ^{213}Bi-labeled CHX-A″-NM3E2 scFv; (C) 0.3 μCi ^{213}Bi-labeled CHX-A″-C6.5K-A scFv; (D) 0.3 μCi ^{213}Bi-labeled CHX-A″-NM3E2 scFv; (E) unlabeled C6.5K-A scFv. Results are presented as percent of initial tumor volume (mm^3).

combination of specific and nonspecific targeting components has advantages over the status quo.

In light of the results presented here, it is clear that more effort must be expended to match the physical half-lives of therapeutic isotopes with the biological properties of their delivery vehicles. For example, with a β half-life (elimination rate from circulation) of 5.7 h and a tumor retention half-life of nearly 24 h, the C6.5 diabody could be effectively paired with either ^{90}Y or ^{211}At, which have half-lives of 64 and 7.2 h, respectively. Furthermore, the best use of the short-lived ^{213}Bi may be in antibody pretargeting applications where the isotope-chelate complexes have elimination half-lives on the order of 30 min.

In conclusion, although scFv-targeted short-lived α emitters can mediated tumor growth delays, the majority of their effects are likely not dependent on the specificity of the targeting vehicle. Utilization of isotopes with half-lives that more closely match the pharmacokinetic and tumor retention profiles of the delivery vehicle should significantly improve the specificity of therapeutic effects.

References

1. Adams G. P., DeNardo S. J., Deshpande S. V., DeNardo G. L., Meares C. F., McCall M. J. and Epstein A. L. (1989) Effect of mass of ^{111}In-benzyl-EDTA monoclonal antibody on hepatic uptake and processing in mice. *Cancer Res.* **49**, 1707–1711.
2. Adams G. P., McCartney J. E., Tai M.-S., Oppermann H., Huston J. S., Stafford W. F., Bookman M. A., Fand I., Houston L. L. and Weiner L. M. (1993) Highly specific *in vivo* tumor targeting by monovalent and divalent forms of 741F8 anti-c-erbB-2 single-chain Fv. *Cancer Res.* **53**, 4026–4034.
3. Adams G. P., Schier R., Marshall K., Wolf E. J., McCall A. M., Marks J. D. and Weiner L. M. (1998) Increased affinity leads to improved selective tumor delivery of single chain Fv antibodies. *Cancer Res.* **58**, 485–490.
4. Adams G. P., Schier R., McCall A. M., Crawford R. S., Wolf E. J., Weiner L. M. and Marks J. D. (1998) Prolonged *in vivo* tumor retention of a human diabody targeting the extracellular domain of human HER2/neu. *Brit. J. Cancer* **77**, 1405–1412.
5. Alpaugh K. and von Mehren M. (1999) Monoclonal antibodies in cancer treatment. *BioDrugs* **3**, 209–236.
6. Behr T. M., Goldenberg D. M. and Becker W. (1998) Reducing renal accretion of radiolabelled antibody fragments and peptides: Improvement of therapeutic efficacy by overcoming nephrotoxic potential? A review. *Tumor Targeting* **3**, 2–12.
7. Behr T. M., Sharkey R. M., Malik J. E., Blumenthal R. D., Dunn R. M., Griffiths G. L., Bair H.-J., Wolf F. G., Becker W. S. and Goldenberg D. M. (1995) Reduction of the renal uptake of radiolabeled monoclonal antibody fragments by cationic amino acids and their derivatives. *Cancer Res.* **55**, 3825–3834.
8. Colcher D. R., Bird R., Roselli M., Hardman K. D., Johnson S., Pope S., Dodd S. W., Pantoliano M. W., Milenic D. E. and Schlom, J. (1990) In vivo tumor targeting of a recombinant single-chain antigen-binding protein. *J. Natl. Cancer Inst.* **82**, 1191–1197.
9. DePalatis L. R., Frazier K. A., Cheng R. C. and Kotite N. J. (1995) Lysine reduces renal accumulation of radioactivity associated with injection of the [^{177}Lu]α-[2-(4-aminophenyl) ethyl]-1,4,7,10-tetraazacyclodecane-1,4,7,10-tetraacetic acid-CC49 immunoconjugate. *Cancer Res.* **55**, 5288–5295.
10. Feinendegen L. E. and McClure J. J. (1997) Alpha-emitters for medical therapy—Workshop of the United States Department of Energy (meeting report) *Radiat. Res.* **148**, 195–201.
11. Feinendegen L. E. and McClure J. J. (1999) Alpha emitters for medical therapy: Second Bi-annual Workshop. Toronto, Canada. June 4–5, 1998. USA Dept. of Energy Publication DOE/NE-0116.
12. Hann H.-W. L., Stahlhut M. W., Rubin R. and Maddrey W. C. (1992) Antitumor effect of deferoxamine on human hepatocellular carcinoma growing in athymic nude mice. *Cancer* **70**, 2025–2056.
13. Hollinger P., Prospero T. and Winter G. (1993) "Diabodies": Small bivalent and bispecific antibody fragments. *Proc. Natl. Acad. Sci. USA* **90**, 6444–6448.
14. Huston J. S., Levinson D., Mudgett-Hunter M., Tai M.-S. and Novotny J. (1988) Protein engineering of antibody binding sites: Recovery of specific activity in an anti-digoxin single-chain Fv analogue produced in *E coli*. *Proc. Natl. Acad. Sci. USA* **85**, 5879–5883.
15. Jain R. K. (1993) Physiological resistance to the treatment of solid tumors. Fourth Annual IBC International Conference on Antibody Engineering. **4**, 87–105.
16. Jain R. K. (1987) Transport of molecules in the tumor interstitum: A review. *Cancer Res.* **47**, 3039–3051.
17. Kaminski M. S., Zasady K. R., Francis I. R., Milik A. W., Ross C. W., Moon S. D., Crawford S. M., Burgess J. M., Petry N. A., Butchko G. M., Glenn S. D. and Wahl R. L. (1993) Radioimmunotherapy of B-cell lymphoma with ^{131}I-anti-B1 (anti-CD20) antibody. *New Engl. J. Med.* **329**, 459–465.
18. Kennel S. J. and Mirzadeh S. (1998) Vascular targeted radioimmunotherapy with ^{213}Bi—an α-particle emitter. *Nucl. Med. Biol.* **25**, 241–246.
19. Knox S. J., Goris M. L., Trisler K., Negrin R., Davis T., Liles T. M., Grillo-Lopez A., Chinn P., Varns C., Ning S. C., Fowler S., Deb N., Becker M., Marquez C. and Levy R. (1996) Yttrium-90-labeled anti-CD20 monoclonal antibody therapy of recurrent B-cell lymphoma. *Clin. Cancer Res.* **2**, 457–470.
20. Kobayashi H., Wu C., Yoo T. M., Sun B. F., Drumm D., Pastan I., Paik C. H., Gansow O. A., Carrasquillo J. A. and Brechbiel M. W. (1998) Evaluation of the *in vivo* biodistribution of yttrium-labeled isomers of CHX-DTPA-conjugated monoclonal antibodies. *J. Nucl. Med.* **39**, 829–836.
21. Macklis R. M., Kinsey B. M., Kassis A. L., Ferrara J. L. M., Atcher R. W., Hines J. J., Coleman C. N., Adelstein S. J. and Burackoff S. J. (1988) Radioimmunotherapy with alpha-emitting immunoconjugates. *Science* **240**, 1024–1026.
22. McDevitt M. R., Sgouros G., Finn R. D., Humm J. L., Jurcic J. G., Larson S. M. and Scheinberg D. A. (1998) Radioimmunotherapy with alpha-emitting nuclides. *Eur. J. Nucl. Med.* **25**, 1341–1351.
23. Meares C. F., McCall M. J., Reardan D. T., Goodwin D. A., Diamanti C. I. and McTigue M. (1984) Conjugation of antibodies with bifunctional chelating agents: Isothiocyanate and bromoacetamide reagents, methods of analysis, and subsequent addition of metal ions. *Anal. Biochem.* **142**, 68–78.
24. Milenic D. E., Yokota T., Filpula D. R., Finkelman M. A. J., Dodd S. W., Wood J. F., Whitlow M., Snoy P. and Schlom J. (1991) Construction, binding properties, metabolism, and targeting of a single-chain Fv derived from the pancarcinoma monoclonal antibody CC49. *Cancer Res.* **51**, 6363–6371.
25. Mirzadah S., Brechbiel M. W., Atcher R. W. and Gansow O. A. (1990) Radiometal labeling of immunoproteins: Covalent linkage of 2-(4-isothiocyanatobenzyl) diethylenetriaminepentaacetic acid ligands to immunoglobulin. *Bioconjug. Chem.* **1**, 59–65.
26. Nikula T. K., McDevitt M. R., Finn R. D., Wu C., Kozak R. W., Garmestani K., Brechbiel M. W., Curcio M. J., Pippin C. G., Tiffany-Jones L., Geerlings M. W. Sr., Apostolidis C., Molinet R., Geerlings M. W. Jr., Gansow O. A. and Scheinberg, D. A. (1999) Alpha-emitting bismuth cyclohexylbenzyl DTPA constructs of recombinant humanized anti-CD33 antibodies: Pharmacokinetics, bioactivity, toxicity and chemistry. *J. Nucl. Med.* **40**, 166–176.
27. Pimm M. V. and Gribben S. J. (1994) Prevention of renal tubule re-absorption of radiometal (indium-111) labelled Fab fragment of a monoclonal antibody in mice by systemic administration of lysine. *Eur. J. Nucl. Med.* **21**, 663–665.
28. Pippin C. G., Parker T. A., McMurry T. J. and Brechbiel M. W. (1992) Spectrophotometric method for the determination of a bifunctional DTPA ligand in DTPA-monoclonal antibody conjugates. *Bioconjug. Chem.* **3**, 342–345.
29. Press O. W., Eary J. F., Appelbaum F. R., Martin P. J., Badger C. C., Nelp W. B., Glenn S., Butchko G., Fisher D., Porter B., Matthews D. C., Fischer L. D. and Bernstein I. D. (1993) Radiolabeled-antibody therapy of B-cell lymphoma with autologous bone marrow support. *New Engl. J. Med.* **329**, 1219–1224.
30. Schier R., Marks J. D., Wolf E. J., Apell G., Wong C., McCartney J. E., Bookman M. A., Huston J. S., Houston L. L., Weiner L. M. and Adams G. P. (1995) *In vitro* and *in vivo* characterization of a human anti-c-erbB-2 single-chain Fv isolated from a filamentous phage antibody library. *Immunotechnology* **1**, 73–81.
31. Schier R., McCall A., Adams G. P., Marshall K. W., Merritt H., Yim M., Crawford R. S., Weiner L. M. and Marks J. D. (1996) Isolation of picomolar affinity anti-c-erbB-2 single-chain Fv by molecular evolution

of the complementarity determining regions in the center of the antibody binding site. *J. Mol. Biol.* **263,** 551–567.
32. Schott M. E., Milenic D. E., Yokota T., Whitlow M., Wood J. F., Fordyce W. A., Cheng R. C. and Schlom J. (1992) Differential metabolic patterns of iodinated versus radiometal chelated anti-carcinoma single-chain Fv molecules. *Cancer Res.* **52,** 6413–6417.
33. Simonson R. B., Ultee M. E., Hauler J. A. and Alvarez V. L. (1990) Radioimmunotherapy of peritoneal human colon cancer xenografts with site-specifically modified Bi-212-labeled antibody. *Cancer Res.* **50,** 985s–988s.
34. Wilbur D. S. (1991) Potential use of alpha emitting radionuclides in the treatment of cancer. *Antibody, Immunoconj. Radiopharm.* **4,** 85–97.
35. Wu A. M., Chen W., Raubitschek A. A., Willams L. E., Fischer R., Hu S.-Z., Odom-Maryon T., Wong J. Y. C. and Shively J. E. (1996) Tumor localization of anti-CEA single chain Fvs: Improved targeting by non-covalent dimers. *Immunotechnology* **2,** 21–36.
36. Wu A. M., Wiliams L. E., Zieran L., Padma A., Sherman M., Bebb G. G., Odom-Maryon T., Wong J. Y. C., Shively J. E. and Raubitschek A. A. (1999) Anti-carcinoembryonic antigen (CEA) diabody for rapid tumor targeting and imaging. *Tumor Targeting* **4,** 47–58.
37. Wu C., Brechbiel M. W. and Gansow O. A. (1997) An improved generator for the production of ^{213}Bi from ^{225}Ac. *Radiochim. Acta* **79,** 141–144.
38. Wu C., Kobayashi H., Sun B., Yoo T. M., Paik C. H., Gansow O. A., Carrasquillo J. A., Pastan I. and Brechbiel M. W. (1997) Stereochemical influence on the stability of radio-metal complexes *in vivo*. Synthesis and evaluation of the four stereoisomers of 2-(*p*-nitrobenzyl)-trans-CyDTPA. *Bioorg. Med. Chem.* **5,** 1925–1934.